A new nonparametric adaptive EWMA control chart with exact run length properties

Anan Tang, Jinsheng Sun, Xuelong Hu, Philippe Castagliola

A New Nonparametric Adaptive EWMA Control Chart with Exact Run Length Properties

January 19, 2019

Anan Tang, School of Automation, Nanjing University of Science and Technology, Nanjing, China. Emai: tanganan2@sina.com;

Jinsheng Sun, School of Automation, Nanjing University of Science and Technology, Nanjing, China. Emai: jssun67@163.com;

Xuelong Hu, School of Management, Nanjing University of Posts and Telecommunications, Nanjing, China. Email: hxl0419@hotmail.com;

Philippe Castagliola (Corresponding Author), Université de Nantes & LS2N UMR CNRS 6004, Nantes, France. Email: philippe.castagliola@univ-nantes.fr.

A New Nonparametric Adaptive EWMA Control Chart with Exact Run Length Properties

immediate

January 19, 2019

Abstract

The AEWMA (Adaptive Exponentially Weighted Moving Average) chart is a scheme that combines the Shewhart and the classical EWMA charts in a smooth way. In this paper, a new nonparametric AEWMA-type chart for count data, based on the sign statistic (denoted as the CAEWMA SN chart), is proposed without requiring any parametric probability distribution for the underlying process. The most valuable characteristics of this work are: i) it combines the advantages of a nonparametric control chart with the best overall shift detection properties of an AEWMA-type chart, ii) only positive integer-valued weights are used for the monitoring of count data, and the plotted statistic is also an integer and iii) an appropriate discrete-time Markov chain technique is provided to compute the *exact* run length properties of the proposed chart without any expensive simulation or unreliable approximation. Detailed guidelines and recommendations for selecting the chart's parameters are provided with two illustrative examples. An extensive comparative study demonstrates the superiority of the CAEWMA SN chart over a number of existing control charts, including a discrete EWMA-type sign chart, two classical continuous EWMA-type charts and a GWMA-type sign chart, for detecting a wide range of location shifts.

Keywords: Adaptive EWMA Sign Chart; Count Data; Distribution-free Chart

1 Introduction

In the field of SPM (Statistical Process Monitoring), control charts have been considered as the most effective technique for monitoring various kind of process characteristics, commonly the process location or scale. The main types of control charts are the Shewhart, the CUSUM (Cumulative Sum) and the EWMA (Exponentially Weighted Moving Average) charts. Most of these charts, however, critically rely on the pre-specified size of the shift. As the practitioner only has a vague information about the magnitude of the actual shift size when the process goes out-of-control, it is generally difficult to exactly pre-determine it in advance. For this reason, instead of trying to define a unique shift size, it could be wiser to simply define a range of potential shift sizes for which the control scheme would be designed to quickly react. With this in mind, Capizzi and Masarotto (2003) have proposed an Adaptive EWMA chart (denoted as AEWMA), for monitoring continuous data, which combines the Shewhart and the classical EWMA schemes in a smooth way. In their study, the smoothing parameter could be seen as a function of the difference between the current observation and the last AEWMA statistic value. A single AEWMA chart could thus be designed for efficiently detecting both a small mean shift $\delta_{\min}$ and a large mean shift $\delta_{\max}(> \delta_{\min})$ simultaneously. Since the adaptive scheme provides an excellent flexibility, it has been updated on several occasions after its inception, see, for instance, Saleh et al. (2013), Aly et al. (2015, 2017) and Tang et al. (2017, 2018a,b).

It is worth noting that the existing control charts are usually designed with a specific parametric model assumption (most commonly the normal distribution) about the population. However, such an assumption should be ideally verified using either exploratory approaches (e.g. graphical) or confirmatory ones (e.g. hypothesis testing). If the underlying process distribution is in doubt or the actual distribution is different from the assumed one, the properties of these parametric charts can be highly affected in such situations. For example, according to Noorossana et al. (2016), the EWMA chart would have an increased false alarm rate for skewed and heavy-tailed distributions. Besides, the effect of parameter estimation on control chart properties is also an important research topic. When the parameters are estimated, the control charts performance is known to differ from the performance of the corresponding chart with known parameters due to the variability of the estimators. Problems that are associated with this are "What is the minimal number of Phase I samples required to ensure an adequate performance in Phase II?" and "How should the Phase II control limits be adjusted to compensate for the insufficient number of Phase I samples?" For example, Saleh et al. (2015) suggested to use 600 samples of size $n = 5$ if $\lambda = 0.1$, 900 samples if $\lambda = 0.5$ and 1000 samples if $\lambda = 1.0$ to reduce the variation in the EWMA $\bar{X}$ chart performance. Therefore, these researches can be of a limited interest as, in practice, the underlying process distribution is often not explicitly known to assume normality (or any specific parametric distribution), and practitioners may not have a sufficient amount of Phase I data to obtain an accurate estimation of the parameter(s).

At this point, it is reasonable for quality practitioners to use nonparametric methods in some situations. The advantages of nonparametric control charts are: i) simplicity, ii) no requirement for a particular distribution, iii) better robustness and outlier resistance and iv) advantage in start-up or short-run situations. Therefore, a nonparametric control chart is a recommended alternative as its in-control properties remain valid for any distributions. The increasing trend of practical uses of nonparametric control charts have been seen, for example, in Chakraborti et al. (2015), Mukherjee and Marozzi (2017) and Triantafyllou (2018). A class of Shewhart-type distribution-free control charts has been considered by Albers and Kallenberg (2004), Bakir (2004), Chakraborti and Eryilmaz (2007), Jones-Farmer et al. (2009) and Human et al. (2010).

On the other hand, nonparametric EWMA-type charts have gained more attention in practice because of their higher ability to react faster against small and moderate shifts in the process parameter(s). A nonparametric EWMA chart using a change-point formulation based on the Mann-Whitney statistic was investigated in Zhou et al. (2009). Li et al. (2010) investigated two nonparametric analogs of the CUSUM and EWMA control charts based on the Wilcoxon rank-sum test. Zou and Tsung (2010) proposed a control chart based on the integration of a powerful nonparametric goodness-of-fit test and the classical EWMA control scheme, which is efficient in detecting potential shifts in location, scale, and shape parameters. Graham et al. (2011) studied a nonparametric EWMA control chart based on the Wilcoxon signed-rank statistic for the location. A two-sided nonparametric Phase II EWMA control chart using the exceedance statistics, has been proposed in Graham et al. (2012). Based on the same exceedance statistics, Graham et al. (2017) further investigated various aspects related to an efficient design and execution issues concerning the nonparametric EWMA control charts previously proposed in Graham et al. (2012). Chakraborty et al. (2016) proposed a distribution-free GWMA control chart based on the Wilcoxon signed-rank statistic and Abid et al. (2017) investigated the performance of an EWMA signed-rank chart using ranked set sampling. Compared with the signed-rank chart, the advantage of the sign chart is that the latter can also be used for an asymmetrical distribution. A new version of the EWMA sign control chart based on an arcsine transformation of the sign statistic has been proposed in Yang et al. (2011). Aslam et al. (2014) proposed a new nonparametric EWMA sign control chart based on the repetitive sampling. Lu (2015) extended Yang et al. (2011)'s study to a nonparametric GWMA sign chart for monitoring deviations from the process target. For more discussion on multivariate sign EWMA

control charts, readers may refer to Zou and Tsung (2011), Zi et al. (2013) and Haq and Khoo (2018).

However, it is important to note that, if nonparametric statistics (like the sign or the Wilcoxon signed-rank statistics) are defined on integer-valued domains, the use of the classical EWMA scheme (with a real-valued smoothing parameter λ) or the classical AEWMA scheme (with a real-valued score function φ) will lead to statistics that are not integer-valued any longer. In this case, the computation of the run length properties relies either on pure simulation techniques or on the use of a discrete time Markov chain after discretization of the control limits interval. The former approach clearly relies on how many simulation runs are randomly generated. For example, Li et al. (2010) suggested a $N = 100,000$ replications to verify the results using Monte Carlo simulations. The second approach, unfortunately, also leads to an unreliable results (ARL for example) as it heavily fluctuates due to the number of states selected for the Markov chain and the discrete nature of the statistic to be monitored, see Weiß (2009), Rakitzis et al. (2015) and Castagliola et al. (2018). In this work, we extend a *discrete* version of the AEWMA scheme introduced by Capizzi and Masarotto (2003) in order to enhance its detection capability for nonparametric statistics. An appropriate Markov chain technique is developed to guarantee *exact results* for the run length distribution, i.e. without any approximation. This simplifies the performance analysis without running a large number of simulations.

The remainder of this paper is organized as follows: Section 2 discusses the idea of the CEWMA SN chart. The proposed CAEWMA SN chart is presented in Section 3. An appropriate discrete-time Markov chain methodology to compute the exact run length properties of the proposed chart is provided in Section 4. Section 5 is concerned with some optimal designs of the CAEWMA SN chart: i) the ARL-based design for the detection of a *specific* magnitude of shift in subsection 5.1 and, ii) the AARL-based design for the detection of a *range* of unknown shifts in subsection 5.2. The in-control robustness is compared to the parametric AEWMA chart for the mean in Section 6. Two illustrative examples are shown in Section 7 and, finally, some conclusions and future researches are given in Section 8.

2 The CEWMA SN control chart

Let us assume that, at time $t = 1, 2, \ldots$, we have a Phase II subgroup $\{X_{t,1}, X_{t,2}, \ldots, , X_{t,n}\}$ of size $n \geq 1$, and $X_{t,j}$ comes from an unknown continuous distribution with c.d.f. (cumulative distribution function) $F_X(x|\theta)$, where θ is the location parameter. Without loss of generality, we consider the sample median θ as the location parameter to be monitored. The process is said to be in-control if $\theta = \theta_0$ and when the process is out-of-control, we have $\theta = \theta_1$. Define the sign statistic

$$\mathrm{SN}_t = \sum_{j=1}^{n} \mathrm{sign}(X_{t,j} - \theta_0), \quad t = 1, 2, \ldots, \tag{1}$$

where

$$\mathrm{sign}(x) = \begin{cases} -1 & \text{if} \quad x < 0 \\ 0 & \text{if} \quad x = 0 \\ 1 & \text{if} \quad x > 0 \end{cases}. \tag{2}$$

The statistic SN_t is linearly related to the statistic T_t through the relationship $\mathrm{SN}_t = 2T_t - n$, where $T_t = \#\{X_{t,j} > \theta_0, j = 1, 2, \ldots, n\}$, i.e. T_t is the number of observations $\{X_{t,1}, X_{t,2}, \ldots, , X_{t,n}\}$ larger than θ_0. Accordingly, the value of SN_t can be a positive or a negative integer in $\{-n, -n+2, \ldots, n-2, n\}$. For an in-control process, i.e. $P(X_{t,j} < \theta_0 | \theta = \theta_0) = P(X_{t,j} > \theta_0 | \theta = \theta_0) = p_0 = 0.5$, the statistic T_t follows a binomial distribution $\mathrm{Bin}(n, 0.5)$. Consequently, monitoring the deviation $\theta = \theta_1$ from the process target is equivalent to monitoring a change in the process proportion $p_1 \neq p_0$. Consequently, monitoring the deviation $\theta = \theta_1$ from the process target is equivalent to monitoring a

change in the process proportion $p_1 \neq p_0$ with $p_1 = P(X_{t,j} > \theta_0 | \theta = \theta_1)$. In this case they are two situations:

- either the change $p_0 \to p_1$ occurs *between subgroups* and, in this case, if the change already happened, T_t simply follows a binomial distribution $\text{Bin}(n, p_1)$ with p.m.f. (probability mass function) $f_{T_t}(t) = f_B(t|n, p_1) = \binom{n}{t} p_1^t (1-p_1)^{n-t}$.
- either the change $p_0 \to p_1$ occurs *within subgroups* and the first n_0 observations $X_{t,1}, X_{t,2}, \ldots, X_{t,n_0}$ are assumed to be in-control while, the last n_1 observations $X_{t,n_0+1}, X_{t,n_0+2}, \ldots, X_{t,n}$ (with $n = n_0 + n_1$) are assumed to be out-of-control. Conquequently, in this case, we have $T_t = T_{t0} + T_{t1}$ where $T_{t0} = \#\{X_{t,j} > \theta_0, j = 1, 2, \ldots, n_0\}$ and $T_{t1} = \#\{X_{t,j} > \theta_0, j = n_0 + 1, n_0 + 2, \ldots, n\}$. This implies that T_t is the sum of two binomial random variables, the first one T_{t0} with parameters (n_0, p_0) and the second one T_{t1} with parameters (n_1, p_1). In this situation, the distribution of T_t is no longer a binomial distribution but its p.m.f. $f_{T_t}(t)$ can nevertheless be obtained for $t = 0, 1, \ldots, n$ as

$$f_{T_t}(t) = \sum_{x=\max(0,t-n_1)}^{\min(n_0,t)} f_B(x|n_0, p_0) f_B(t-x|n_1, p_1).$$

For simplicity, all the results in this paper will assume the first situation (shifts occur between subgroups) for which T_t follows a binomial distribution. The second situation (shifts occur within subgroups) will not be investigated in the paper. Notably, we only consider the SN chart to monitor location shifts. However, the proposed technique can also work exactly the same for any other nonparametric statistics like, for instance, the Wilcoxon signed-rank statistic for the location, see Graham et al. (2011) or the Ansari-Bradley statistic for the dispersion, see Gibbons and Chakraborti (2010).

The plotting statistic $\{Y_1, Y_2, \ldots\}$ of the classical continuous EWMA chart is obtained by sequentially accumulating the sign statistics $\{\text{SN}_1, \text{SN}_2, \ldots\}$ and it is defined as $Y_t = (1-\lambda)Y_{t-1} + \lambda \text{SN}_t$, where $\lambda \in (0, 1]$ is a real valued smoothing constant (i.e. a fixed weight). However, it is important to note that, by applying the classical EWMA chart, the values of the statistic Y_t are not integers anymore, and the results (ARL for instance) obtained by using the Markov chain method are only approximations, which does not necessarily monotonically converge as the number of the Markov chain states increases. This fact was also emphasized by Weiß (2009). At this point, Rakitzis et al. (2015) proposed the new CEWMA monitoring technique for count data, in which not only the observations but also the EWMA statistic Y_t are all integers. Furthermore, Castagliola et al. (2018) extend this idea for monitoring the sequence $\{\text{SN}_1, \text{SN}_2, \ldots\}$ (denoted as CEWMA SN) using the following formula

$$(\gamma_X + \gamma_Y) Y_t + R_t = \gamma_X \text{SN}_t + \underbrace{\gamma_Y Y_{t-1} + R_{t-1}}_{B_{t-1}}, \tag{3}$$

where $(\gamma_X, \gamma_Y) \in \mathbb{N}^2$ are two positive integer-valued parameters to be fixed, $B_{t-1} \overset{\text{def}}{=} \gamma_Y Y_{t-1} + R_{t-1}$, Y_t is the quotient of the Euclidean division

$$Y_t = \left\lfloor \frac{\gamma_X \text{SN}_t + B_{t-1}}{\gamma_X + \gamma_Y} \right\rfloor, \tag{4}$$

where $\lfloor \ldots \rceil$ denotes the rounded towards zero integer (i.e. $\lfloor 3.5 \rceil = 3$ and $\lfloor -3.5 \rceil = -3$, for instance) and $R_t \in \{-\gamma_X - \gamma_Y + 1, \ldots, \gamma_X + \gamma_Y - 1\}$ is the remainder of this Euclidean division, i.e.

$$R_t = \gamma_X \text{SN}_t + B_{t-1} - (\gamma_X + \gamma_Y) Y_t. \tag{5}$$

It is important to note that the values $R_1, R_2, \ldots$ just need to be computed but they are not monitored. Only the values $Y_1, Y_2, \ldots$ are monitored. For more details about the CEWMA chart and the CEWMA SN chart, the interested reader can refer to Rakitzis et al. (2015) and Castagliola et al. (2018).

3 The CAEWMA SN control chart

The CEWMA SN chart proposed in Castagliola et al. (2018) uses a pair of integer-valued constants (γ_X, γ_Y) that can be designed in order to optimally detect a *specific* magnitude of the shift. However, in practice, it is quite difficult to pre-determine the exact size of the shift. A natural option is to find a potential tendency presented in the data and translate it in a time-varying weight. Therefore, to provide a robustness to various magnitudes of shifts in count data, motivated by Capizzi and Masarotto (2003), we propose the following new adaptive EWMA (denoted as CAEWMA SN) scheme for count data

$$\underbrace{(\gamma_X + \gamma_Y)Y_t + R_t}_{C_t} = \varphi(e_t) + \underbrace{(\gamma_X + \gamma_Y)Y_{t-1} + R_{t-1}}_{C_{t-1}}, \tag{6}$$

where $\varphi(e_t) = \varphi(\mathrm{SN}_t - Y_{t-1})$ is a score function and $C_t \overset{\text{def}}{=} (\gamma_X + \gamma_Y)Y_t + R_t$. The term Y_t is the quotient of the Euclidean division

$$Y_t = \left\lfloor \frac{\varphi(\mathrm{SN}_t - Y_{t-1}) + C_{t-1}}{\gamma_X + \gamma_Y} \right\rfloor, \tag{7}$$

where $\lfloor \ldots \rceil$ also denotes the rounded towards zero integer and $R_t \in \{-\gamma_X - \gamma_Y + 1, \ldots, \gamma_X + \gamma_Y - 1\}$ is equal to

$$R_t = \varphi(\mathrm{SN}_t - Y_{t-1}) + C_{t-1} - (\gamma_X + \gamma_Y)Y_t. \tag{8}$$

Particularly, note that the value of Y_{t-1} can also be rewritten as

$$Y_{t-1} = \left\lfloor \frac{C_{t-1}}{\gamma_X + \gamma_Y} \right\rfloor. \tag{9}$$

This definition allows to use the information contained in Y_{t-1} when we define the transient states C_{t-1} of the discrete-time Markov chain (for more details refer to Section 4). When the initial values $Y_0 = y_0$, $R_0 = r_0$ are defined and, the current values SN_t, Y_{t-1}, R_{t-1} as well as the score function $\varphi(e_t)$ are fixed, both Y_t and R_t are uniquely defined. It goes without saying that the error terms e_t between SN_t and Y_{t-1} are also integers, so a new score function, similar to the Huber's score function, has to be proposed here. This score function is defined as

$$\varphi(e) = \begin{cases} e(\gamma_X + \gamma_Y) + k\gamma_Y & \text{if } e < -k \\ e\gamma_X & \text{if } |e| \leq k \\ e(\gamma_X + \gamma_Y) - k\gamma_Y & \text{if } e > k \end{cases}, \tag{10}$$

where k is also a positive integer-valued parameter. Note that:

- when $k \to \infty$, $\varphi(e) = e\gamma_X$. In that case, replacing $\varphi(e)$ by $e\gamma_X = (\mathrm{SN}_t - Y_{t-1})\gamma_X$ in (6) gives $(\gamma_X + \gamma_Y)Y_t + R_t = \gamma_X \mathrm{SN}_t + \gamma_Y Y_{t-1} + R_{t-1}$ and the proposed scheme coincides with the CEWMA SN chart of Castagliola et al. (2018);

- when $k = 0$, $\varphi(e) = e(\gamma_X + \gamma_Y)$. In this case the CAEWMA SN chart reduces to a ordinary Shewhart SN chart.

Therefore, the CAEWMA scheme can be regarded as a smooth combination of the Shewhart and the CEWMA schemes. Concerning the initial values y_0 and r_0, a natural choice is $y_0 = E(\mathrm{SN}_t) = 0$ and $r_0 = 0$. While, if a head-start feature is desired, any choice of $y_0 \neq 0$ or $r_0 \neq 0$ can be considered. The process is considered to be out-of-control whenever Y_t exceeds the control limit $(-h, h)$, where $h > 0$ is a positive integer value to be fixed.

4 Run length properties

Control charts are generally evaluated in terms of their RL (Run length) distributions, where the RL represents the number of samples plotted on the control chart before a signal is declared, i.e. $\mathrm{RL} = \inf\{t \geq 1 | Y_t \leq -h \text{ or } Y_t \geq h\}$. Let $\mathbf{Q}$ be the $(2m+1, 2m+1)$ matrix of probabilities $q_{i,j}$ corresponding to the $2m+1$ transient states, i.e.

$$\mathbf{Q} = \begin{pmatrix} q_{-m,-m} & \cdots & q_{-m,-1} & q_{-m,0} & q_{-m,1} & \cdots & q_{-m,m} \\ \vdots & \vdots & \vdots & \vdots & \vdots & \vdots & \vdots \\ q_{-1,-m} & \cdots & q_{-1,-1} & q_{-1,0} & q_{-1,1} & \cdots & q_{-1,m} \\ q_{0,-m} & \cdots & q_{0,-1} & q_{0,0} & q_{0,1} & \cdots & q_{0,m} \\ q_{1,-m} & \cdots & q_{1,-1} & q_{1,0} & q_{1,1} & \cdots & q_{1,m} \\ \vdots & \vdots & \vdots & \vdots & \vdots & \vdots & \vdots \\ q_{m,-m} & \cdots & q_{m,-1} & q_{m,0} & q_{m,1} & \cdots & q_{m,m} \end{pmatrix}. \tag{11}$$

The RL distribution is determined by the transition probability matrix $\mathbf{Q}$ and the initial probability vector $\mathbf{s}$, which can be represented by a $(2m+1, 1)$ vector $\mathbf{s} = (s_{-m}, \ldots, s_{-1}, s_0, s_1, \ldots, s_m)$. Since the RL is a Discrete Phase-type (DPH) random variable of parameters $(\mathbf{Q}, \mathbf{s})$, the p.d.f. $f_{\mathrm{RL}}(\ell|\mathbf{Q}, \mathbf{s})$ and the c.d.f. $F_{\mathrm{RL}}(\ell|\mathbf{Q}, \mathbf{s})$ of the run length distribution of the CAEWMA SN chart can be easily obtained as:

$$f_{\mathrm{RL}}(\ell|\mathbf{Q}, \mathbf{s}) = \mathbf{s}^\intercal \mathbf{Q}^{\ell-1}(\mathbf{I} - \mathbf{Q})\mathbf{1}, \tag{12}$$

$$F_{\mathrm{RL}}(\ell|\mathbf{Q}, \mathbf{s}) = 1 - \mathbf{s}^\intercal \mathbf{Q}^{\ell}\mathbf{1}, \tag{13}$$

where $\mathbf{I}$ is the $(2m+1, 2m+1)$ identity matrix and $\mathbf{1}$ is a $(2m+1, 1)$ vector of 1's. Although there is no simple formula for the central moment $\mu_i = E\left((\mathrm{RL} - E(\mathrm{RL}))^i\right)$ of order $i \geq 1$ of a DPH random variable RL, there is a simple formula for the factorial moment $\nu_i = E(\mathrm{RL}(\mathrm{RL}-1)\ldots(\mathrm{RL}-i+1))$ of order i, which is given by

$$\nu_i = i! \mathbf{s}^\intercal (\mathbf{I} - \mathbf{Q})^{-i} \mathbf{Q}^{i-1} \mathbf{1}. \tag{14}$$

Specifically, when $i = 1, 2$, we may easily conclude that

$$\nu_1 = \mathbf{s}^\intercal (\mathbf{I} - \mathbf{Q})^{-1} \mathbf{1}, \tag{15}$$

$$\nu_2 = 2\mathbf{s}^\intercal (\mathbf{I} - \mathbf{Q})^{-2} \mathbf{Q}\mathbf{1}. \tag{16}$$

Now, we can easily establish a compact formula for the mean $\mathrm{ARL} = E(\mathrm{RL})$ and the standard deviation $\mathrm{SDRL} = \sigma(\mathrm{RL})$ of the RL distribution, that is

$$\mathrm{ARL} = \nu_1, \tag{17}$$

$$\mathrm{SDRL} = \sqrt{\nu_2 - \nu_1^2 + \nu_1}. \tag{18}$$

Particularly, in order to perform the previous computations of the RL properties, we need to know the elements of matrix $\mathbf{Q}$ and vector $\mathbf{s}$. Let us assume that the process is in the in-control state at time $t-1$. For the CEWMA SN chart, Rakitzis et al. (2015) and Castagliola et al. (2018) suggested to define the transient states of the discrete-time Markov chain as the integers $b_{t-1} = \gamma_Y y_{t-1} + r_{t-1}$ with $y_{t-1} \in \{-h+1, \ldots, h-1\}$ and $r_{t-1} \in \{-\gamma_X - \gamma_Y + 1, \ldots, \gamma_X + \gamma_Y - 1\}$. The possible states of the Markov chain are $i \in \{-b, -b+1, \ldots, b\}$ with $b = b_{\max} = -b_{\min} = \gamma_X + h\gamma_Y - 1$, and the total number of transient states is $2m+1 = 2b+1 = 2(\gamma_X + h\gamma_Y - 1) + 1$. Therefore, given that the Markov chain is in state i at time $t-1$, for each value $\mathrm{SN}_t \in \{-n, -n+2, \ldots, n-2, n\}$, we can obtain y_t and r_t using (4) and (5). If $-h < y_t < h$, then the Markov chain moves to the transient state $j = \gamma_Y y_t + r_t$ with a probability $f_B(\frac{\mathrm{SN}_t+n}{2}|n,p)$. If $y_t \leq -h$ or $y_t \geq h$, the process is considered as out-of-control and the potential assignable cause(s) must be found and removed.

However, for the proposed CAEWMA SN chart, the information of y_{t-1} is also needed when the Markov chain is in state i at time $t-1$. Moreover, we notice that, once the state $i \in \{b_{\min}, b_{\min}+1, \ldots, b_{\max}\}$ is defined, the values of y_{t-1} and r_{t-1} are not uniquely determined. For example, when $\gamma_X = 4$, $\gamma_Y = 6$ and $h = 5$, then $y_{t-1} \in \{-4, \ldots, 4\}$, $r_{t-1} \in \{-9, \ldots, 9\}$ and $b_{\max} = -b_{\min} = \gamma_X + h\gamma_Y - 1 = 33$. This implies that $i = \gamma_Y y_{t-1} + r_{t-1} = 25 \in \{-33, \ldots, 33\}$ and the combination can consist of either $y_{t-1} = 4$ and $r_{t-1} = 1$ or $y_{t-1} = 3$ and $r_{t-1} = 7$. Consequently, the CAEWMA sequence of plotting statistics $Y_1, Y_2, \ldots$ is designed as in (6) and we define the set of states $c_{t-1} = (\gamma_X + \gamma_Y) y_{t-1} + r_{t-1}$ for $y_{t-1} \in \{-h+1, \ldots, h-1\}$ and $r_{t-1} \in \{-\gamma_X - \gamma_Y + 1, \ldots, \gamma_X + \gamma_Y - 1\}$. As the minimum value of c_{t-1} is $c_{\min} = (\gamma_X + \gamma_Y)(-h+1) - \gamma_X - \gamma_Y + 1 = -h(\gamma_X + \gamma_Y) + 1$ and the maximum one is $c_{\max} = (\gamma_X + \gamma_Y)(h-1) + \gamma_X + \gamma_Y - 1 = h(\gamma_X + \gamma_Y) - 1$, then all the states of the discrete-time Markov chain at time $t-1$ for the CAEWMA SN chart are $i \in \{-c, -c+1, \ldots, c\}$ with $c = c_{\max} = -c_{\min}$, and the total number of transient states is $2m+1 = 2c+1 = 2(h(\gamma_X + \gamma_Y) - 1) + 1$. At time $t-1$, for $\forall i \in \{-c, -c+1, \ldots, c\}$, from (9) the unique values of $y_{t-1} = \left\lfloor \frac{i}{\gamma_X + \gamma_Y} \right\rceil$ and $r_{t-1} = i - (\gamma_X + \gamma_Y) y_{t-1}$ can be determined. For the same example, when $\gamma_X = 4$, $\gamma_Y = 6$ and $h = 5$, then $y_{t-1} \in \{-4, \ldots, 4\}$, $r_{t-1} \in \{-9, \ldots, 9\}$ and $c_{\max} = -c_{\min} = h(\gamma_X + \gamma_Y) - 1 = 49$. This implies that $i = 25 \in \{-49, \ldots, 49\}$, and the unique correspondence is $y_{t-1} = 2$ and $r_{t-1} = 5$ for $(\gamma_Y + \gamma_X) y_{t-1} + r_{t-1} = 25$.

(Please insert Table 1 here)

A detailed example on how to implement this discrete-time Markov chain approach for a CAEWMA SN chart is now presented. Table 1 shows the structure of the matrix $\mathbf{Q}$ for the case $n = 10$, $h = 3$, $\gamma_X = 1$, $\gamma_Y = 3$ and $k = 10$. It should be noted that the matrix presented in Table 1 is not the actual matrix $\mathbf{Q}$ but only its structure, i.e. for a better visualization, we use the values of SN_t to represent the probabilities $q_{i,j} = f_B(\frac{\mathrm{SN}_t+n}{2}|n,p)$ and we use the "." to represent the positions where the probabilities $q_{i,j} = 0$. For instance, all the "-6" should be replaced by the probability $f_B(\frac{-6+10}{2}|10,p) = f_B(2|10,p)$ and all the "6" should be replaced by the probability $f_B(\frac{6+10}{2}|10,p) = f_B(8|10,p)$. According to the definition, we have $2m+1 = 2(h(\gamma_X + \gamma_Y) - 1) + 1 = 2 \times (3 \times (1+3) - 1) + 1 = 23$ transient states $i, j \in \{-11, -10, \ldots, 11\}$. In order to explain how the algorithm presented above works, let us start by the first case $i = -11$. For this value, we have $y_{t-1} = \left\lfloor \frac{i}{\gamma_X + \gamma_Y} \right\rceil = -2$. Now, depending on the value of SN_t, we have:

- If $\mathrm{SN}_t \in \{-10, -8, -6, -4\}$, then $-k \leq e_t \in \{-8, -6, -4, -2\} \leq k(=10)$, so $\varphi(e_t) = e_t \gamma_X \in \{-8, -6, -4, -2\}$ and $y_t = \left\lfloor \frac{\varphi(e_t)+i}{\gamma_X + \gamma_Y} \right\rceil = \{-4, -4, -3, -3\}$, respectively. As $y_t \leq -h(=-3)$, the process moves to the absorbing state.

- If $\mathrm{SN}_t = -2$, then $-10 \leq e_t = 0 \leq 10$, so $\varphi(e_t) = e_t\gamma_X = 0$ and $y_t = \left\lfloor \frac{0+(-11)}{4} \right\rceil = -2$. As $-3 < y_t < 3$, we have $r_t = \varphi(e_t) + i - (\gamma_X + \gamma_Y)y_t = 0 + (-11) - (1+3) \times (-2) = -3$, and the process moves to the transient state $j = (\gamma_X + \gamma_Y)y_t + r_t = (1+3) \times (-2) + (-3) = -11$ with a probability $q_{i,j} = f_B(\frac{\mathrm{SN}_t+n}{n}|n,p) = f_B(\frac{-2+10}{2}|n,p) = f_B(4|10,p)$.

- If $\mathrm{SN}_t = 0$, then $-10 \leq e_t = 2 \leq 10$, so $\varphi(e_t) = e_t\gamma_X = 2$ and $y_t = \left\lfloor \frac{2+(-11)}{4} \right\rceil = -2$. As $-3 < y_t < 3$, we have $r_t = 2+(-11)-(1+3)\times(-2) = -1$, and the process moves to the transient state $j = (1+3) \times (-2) + (-1) = -9$ with a probability $q_{i,j} = f_B(\frac{0+10}{2}|n,p) = f_B(5|10,p)$.

  $\vdots$

- If $\mathrm{SN}_t = 10$, then $e_t = 12 > 10$, so $\varphi(e_t) = e_t(\gamma_X + \gamma_Y) - k\gamma_Y = 12 \times (1+3) - 10 \times 3 = 18$ and $y_t = \left\lfloor \frac{18+(-11)}{4} \right\rceil = 1$. As $-3 < y_t < 3$, we have $r_t = 18 + (-11) - (1+3) \times 1 = 3$, and the process moves to the transient state $j = (1+3) \times (1) + 3 = 7$ with a probability $q_{i,j} = f_B(\frac{10+10}{2}|n,p) = f_B(10|10,p)$.

More details about the algorithm can be seen in Appendix 1. Finally, the initial probability vector $\mathbf{s} = (s_{-m}, \ldots, s_{-1}, s_0, s_1, \ldots, s_m)$ contains the probabilities that the Markov chain starts in a given state. We set 1 in the entry corresponding to $(\gamma_X + \gamma_Y)y_0 + r_0$ and 0 in the remaining ones. If $y_0 = r_0 = 0$ (no head-start feature), then we have $s_0 = 1$ and $s_i = 0$ for $i \in \{-m, \ldots, -1, 1, \ldots, m\}$. Once the matrix $\mathbf{Q}$ and the vector $\mathbf{s}$ are defined, we can easily obtain the RL properties of the CAEWMA SN chart. Note also that the proposed algorithm works exactly the same for any other discrete distributions with some trivial modifications, i.e. in the determination of the transient probability $q_{i,j}$, the p.m.f. $f_B(\ldots|n,p)$ of the binomial distribution must be replaced by the proper p.m.f.

It is also important to note that, even if the CAEWMA SN chart can be *theoretically* used with a relatively small sample size $n \in \{2, \ldots, 7\}$, it is *practically* impossible to design it in order to guarantee an acceptable and sufficiently large in-control *ARL* like $ARL_0 = 200$, 370.4 or 500, as for most control charts unless n is sufficiently large. For instance, Chakraborti et al. (2011) and Castagliola et al. (2018) have shown that the sample size $n \geq 9$ in order to be able to obtain a sufficiently large in-control, industry standard, ARL value.

5 Design of the CAEWMA SN scheme

The ARL (Average Run Length) is the most widely used index to evaluate the efficiency of control charts. For a fair comparison, the same ARL_0 value is usually taken when the process is in-control ($p = p_0 = 0.5$) and, when the process is out-of-control ($p = p_1 \neq p_0$), the smaller the ARL_1 value, the better the performance of the control chart. Therefore, the optimization of a CAEWMA SN chart consists in finding the combination $(h^*, \gamma_X^*, \gamma_Y^*, k^*)$ that gives the minimum ARL_1 or AARL_1 (Average ARL_1) based on a given ARL_0. This combination can be obtained using the following two steps procedure:

1. Firstly, we have to search for the parameters combinations $(h, \gamma_X, \gamma_Y, k)$ that yield the desired in-control ARL_0. Note that, because of the discreteness of the monitoring statistic Y_t, $\mathrm{ARL}(h, \gamma_X, \gamma_Y, k, n, p_0) = \mathrm{ARL}_0$ cannot be always exactly achieved. Hence, to satisfy $\mathrm{ARL}(h, \gamma_X, \gamma_Y, k, n, p_0) \approx \mathrm{ARL}_0$, only the combinations $(h, \gamma_X, \gamma_Y, k)$ with a value of $\left|\frac{\mathrm{ARL}(h,\gamma_X,\gamma_Y,k,n,p_0)-\mathrm{ARL}_0}{\mathrm{ARL}_0}\right| \leq \zeta$ will be considered, where ζ is a pre-specified threshold.

2. Secondly, among these combinations, some optimal combinations $(h^*, \gamma_X^*, \gamma_Y^*, k^*)$ can be selected for providing an optimal ARL_1 value for a specific shift p_{opt} (subsection 5.1) or an optimal AARL_1 value for a range of unknown shifts Ω_{opt} (subsection 5.2). In order to find the optimal combination $(h^*, \gamma_X^*, \gamma_Y^*, k^*)$ for fixed values of n and p_{opt} or Ω_{opt}, we used an exhaustive search methodology based on the algorithm in Appendix 2.

In the rest of this paper, $\text{ARL}_0 = 370.4$ and $\zeta = 0.05$ will be considered. Moreover, since for the sign chart we have $\text{ARL}(h, \gamma_X, \gamma_Y, k, n, p_1) = \text{ARL}(h, \gamma_X, \gamma_Y, k, n, 1 - p_1)$, it is only necessary to investigate the case $p_1 \in (0, 0.5)$, in which a value of p_1 close to $p_0 = 0.5$ corresponds to a "small" shift, while a value of p_1 close to 0 corresponds to a "large" shift from the target value.

5.1 Properties for detecting a specific magnitude of shift

Most control charts are effective in detecting the shift of a particular size p_{opt}. For example, Shewhart-type charts are efficient in detecting large shifts, and EWMA-type charts can be constructed to perform well for either detecting small or large shifts. Small values of the smoothing parameter λ are used to quickly detect small shifts, while large values are used to efficiently signal the occurrence of large shifts. This is also consistent with the results of the CEWMA SN chart in Castagliola et al. (2018), where the smoothing ratio $\frac{\gamma_X}{\gamma_X+\gamma_Y}$ can be viewed as the classical real smoothing parameter λ. For the CAEWMA SN chart, the ARL-based design is aimed at selecting the optimal combination $(h^*, \gamma_X^*, \gamma_Y^*, k^*)$ such that

$$(h^*, \gamma_X^*, \gamma_Y^*, k^*) = \underset{(h,\gamma_X,\gamma_Y,k)}{\text{argmin}} \ \text{ARL}(h, \gamma_X, \gamma_Y, k, n, p_{\text{opt}}), \tag{19}$$

subject to

$$\text{ARL}(h^*, \gamma_X^*, \gamma_Y^*, k^*, n, p_0) \approx \text{ARL}_0. \tag{20}$$

Here, in order to investigate the optimal out-of-control values ARL_1 for a specific value of the shift p_{opt} and to help practitioners in the implementation of the CAEWMA SN chart, in Table 2, we exhibit some optimal combinations $(h^*, \gamma_X^*, \gamma_Y^*, k^*)$ (first line of each block) for specified shifts $p_{\text{opt}} \in \{0.05, 0.1, \ldots, 0.45\}$, along with the out-of-control $(\text{ARL}_1, \text{SDRL}_1)$ (second line) for $n \in \{10, \ldots, 25\}$. Moreover, as a comparison, the minimum out-of-control $(\text{ARL}_1, \text{SDRL}_1)$ (third line) of the CEWMA SN chart are also presented. As an example, if the desired in-control $\text{ARL}_0 = 370.4$ and the exact shift is $p_{\text{opt}} = 0.4$, from Table 2, when the sample size is $n = 10$, the optimal combination of parameters $(h^*, \gamma_X^*, \gamma_Y^*, k^*)$ of the CAEWMA SN chart is $(2, 9, 113, 10)$, giving the smallest possible out-of-control ARL_1 of 20.1. For the same case, the minimum ARL_1 value for the CEWMA SN chart is $\text{ARL}_1 = 24.8$.

(Please insert Table 2 here)

Through the results in Table 2, the following conclusions are observed:

- As expected, when the sample size n increases, the optimal out-of-control ARL_1 decreases. For example, when $p_{\text{opt}} = 0.45$, as n increases from 10 to 15, the minimum ARL_1 value decreases from 53.2 to 39.1 for the CAEWMA SN chart, and it decreases from 61.1 to 42.4 for the CEWMA SN chart.

- Given a fixed value of n, the larger the value of p_{opt}, the smaller the smoothing ratio $\frac{\gamma_X^*}{\gamma_X^*+\gamma_Y^*}$. For example, when $n = 16$, we have $\frac{\gamma_X^*}{\gamma_X^*+\gamma_Y^*} = \frac{7}{7+9} \approx 0.44$ for $p_{\text{opt}} \in \{0.05, 0.10, 0.15\}$, $\frac{\gamma_X^*}{\gamma_X^*+\gamma_Y^*} =$

$\frac{9}{9+25} \approx 0.26$ for $p_{\text{opt}} = 0.30$ and $\frac{\gamma_X^*}{\gamma_X^*+\gamma_Y^*} = \frac{5}{5+93} \approx 0.05$ for $p_{\text{opt}} = 0.45$. This is consistent with the results of EWMA-type charts as investigated in Yang et al. (2011) and Castagliola et al. (2018).

- The CAEWMA SN chart outperforms the CEWMA SN chart when the sample size is small $n \leq 15$. This is especially true for large shifts (i.e. $p_{\text{opt}} \leq 0.15$) and small shift (i.e. $p_{\text{opt}} \geq 0.40$). For example, when $n = 10$, the CEWMA SN chart has the minimum $\text{ARL}_1 = 2.2$ for $p_{\text{opt}} = 0.05$ and the minimum $\text{ARL}_1 = 61.1$ for $p_{\text{opt}} = 0.45$. While the minimum ARL_1 values of the CAEWMA SN chart for $p_{\text{opt}} = \{0.05, 0.45\}$ are 1.4 and 53.2, respectively. As soon as n becomes larger, the performance of the CAEWMA SN and CEWMA SN charts are nearly the same.

In conclusion, if the exact size of the shift can be pre-determined, the superiority of the CAEWMA scheme is not so significant. However, in practice, the problem is that this "optimal" scheme strongly depends on the specified magnitude of the shift p_{opt}, but specifying the exact shift size could be too restrictive as practitioners may not have a historical knowledge of the process. In this case, the control chart based on the minimum ARL_1 strategy, for a specified shift p_{opt}, will be seriously affected if a different shift size actually occurs in practice. As a consequence, it seems that a scheme, which can offer a reasonable protection for both small and large shifts simultaneously, is a best choice.

5.2 Properties for detecting a range of unknown shifts

An alternative approach to design a control chart is to optimize its performance for a whole range of shifts Ω_{opt} rather than for one or two particular shifts. As AEWMA-type schemes are smooth combination of Shewhart-type and EWMA-type schemes, they have an advantage over the EWMA-type schemes which can only be designed to detect either small or large shifts, and over the Shewhart-type schemes which are known to be insensitive to small shifts. Thus, an optimal design based on a whole range of shifts is more reasonable for the CAEWMA SN chart to achieve a good AARL performance.

If we assume that $f_{p_1}(p)$ is the p.d.f. of the shift p_1 over the range Ω_{opt}, and $\omega_{p_1}(p)$ is a nonnegative function representing the weight associated to p_1 then, the AARL-based design of the CAEWMA SN chart has the following form:

$$(h^*, \gamma_X^*, \gamma_Y^*, k^*) = \underset{(h,\gamma_X,\gamma_Y,k)}{\text{argmin}} \ \text{AARL}(h, \gamma_X, \gamma_Y, k, n, \Omega_{\text{opt}}), \tag{21}$$

subject to

$$\text{ARL}(h^*, \gamma_X^*, \gamma_Y^*, k^*, n, p_0) \approx \text{ARL}_0, \tag{22}$$

with

$$\text{AARL} = \int_{\Omega_{\text{opt}}} \omega_{p_1}(p)\text{ARL}(h, \gamma_X, \gamma_Y, k, n, p) f_{p_1}(p)\text{d}p. \tag{23}$$

As practitioners do not have a specific preference concerning the actual shape of the shift distribution, we assumed that the shift follows a discrete uniform distribution $f_{p_1}(p) \sim U[p_{\min}, p_{\max}]$, where $p_{\min}$ and $p_{\max}$ are the lower and upper bounds of the shift, respectively. Concerning the weight functions $\omega_{p_1}(p)$, there are no specific rule for choosing it. It just helps to avoid over-correction against small shifts (because the ARL_1 values for small shifts are quite larger than that for large shifts). In this paper, we assume a weight function $\omega_{p_1}(p) = \frac{1}{p}$. Other weight functions can be discussed in a similar way, and interested readers can refer to Ou et al. (2012) and Aly et al. (2017) for more details.

(Please insert Table 3 here)

Table 3 displays some optimal parameters of CAEWMA SN charts obtained using the above strategy based on a whole range of shifts $\Omega_{\text{opt}} = \{0.05, 0.10, \ldots, 0.45\}$. To evaluate the properties for various shifts, the RMI (Relative Mean Index) proposed by Han and Tsung (2006) is used and it is defined as follows:

$$\text{RMI}(T) = \frac{1}{N}\sum_{i=1}^{N}\left(\frac{\text{ARL}(T, p_1^{(i)}) - \text{ARL}^*(p_1^{(i)})}{\text{ARL}^*(p_1^{(i)})}\right), \tag{24}$$

where $\text{ARL}(T, p_1^{(i)})$ denotes the ARL value of the control chart T when detecting the shift $p_1^{(i)}$, and $\text{ARL}^*(p_1^{(i)})$ is the minimum ARL value of all charts compared when detecting $p_1^{(i)}$, where $p_1^{(i)}$ is the i^{th} shift and N is the number of shifts considered in the comparison (for example, if $p_1 \in \{0.05, 0.10, \ldots, 0.45\}$ then $N = 9$ and $p_1^{(1)} = 0.05, \ldots, p_1^{(9)} = 0.45$). So $\text{RMI}(T)$ can be considered as a relative efficiency measure of the given control charts, compared with the best chart, when detecting the shift $p_1^{(i)}$. Obviously, a smaller value for $\text{RMI}(T)$ means that the control chart T has a better performance for detecting shifts on the whole.

In Tables 4 to 7, we compare the ARL and RMI performance of the CAEWMA SN chart, with the standard and the arcsine transformed EWMA SN charts of Yang et al. (2011), the GWMA SN chart of Lu (2015) as well as the CEWMA SN chart of Castagliola et al. (2018). Note that, the ARL values of the GWMA SN can be computed only via simulations while, for others, the Markov chain approach can be applied.

Comparisons with the EWMA SN **chart**

The standard (denoted as EWMA-S) and the arcsine transformed (denoted as EWMA-A) EWMA SN charts proposed in Yang et al. (2011) were calculated for various values of (k^*, λ^*) for the subgroup size $n \in \{9, 10, \ldots, 25\}$. These combinations correspond to an ARL_0 close to the standard of 370.4. Tables 4 and 5 compare respectively the ARL values of the CAEWMA SN chart with the EWMA-S and EWMA-A charts when $n = 20$. Agreeing with the recommendations in Table 1 of Yang et al. (2011), the EWMA SN charts are designed with five values of λ (i.e. $0.05, 0.15, 0.3, 0.6, 0.9$) and the considered CAEWMA SN chart is designed for $\Omega_{\text{opt}} = \{0.05, 0.10, \ldots, 0.45\}$, i.e.$(h^*, \gamma_X^*, \gamma_Y^*, k^*) = (4, 4, 23, 14)$, as shown in Table 3 when $n = 20$.

(Please insert Tables 4 to 5 here)

We found that, for both EWMA-S and EWMA-A charts, small values of λ could help in detecting small shifts more quickly, and large values of λ could help in detecting larger shifts faster. This means that a single EWMA SN (regardless EWMA-S or EWMA-A) chart can be designed to detect either small or large shifts effectively, but not both simultaneously. For example, in Table 4, if the EWMA-S chart, with $\lambda = 0.05$, can be efficient in the detection of small shifts (e.g. $p_1 = 0.45$), it is unfortunately insensitive to moderate or large ones (e.g. $p_1 \leq 0.3$). Moreover, it can be found that, both the EWMA-S and EWMA-A charts can just provide a slightly better performance than the CAEWMA SN chart when the shift size is close to the value for which they have been optimized. For other shift sizes, the CAEWMA SN chart also provides additional protection, even if the actual shift is very different from its specified size. For instance, in Table 5, the EWMA-A chart with $\lambda = 0.05$ achieves the minimum $\text{ARL}_1 = 31.0$ for $p_1 = 0.45$ followed by the $\text{ARL}_1 = 36.6$ of the CAEWMA SN chart, while for $p_1 \leq 0.4$, the CAEWMA SN chart performs much better than the EWMA-A chart with a $\lambda = 0.05$.

Comparisons with the GWMA SN **chart**

Table 6 is similar to Tables 4 and 5 but with the EWMA SN charts replaced by the GWMA SN chart. The run length distribution of the GWMA SN chart is a function of (L, q, α), where L denotes the width of the control limit, q is the weight parameter and α is a parameter to adjust the kurtosis of the weighting function. For a fixed value of α, a large value of q of the GWMA SN chart is highly sensitive in detecting small shifts. The optimal combinations $(2.929, 0.4, 0.6)$, $(2.925, 0.6, 0.9)$, $(2.771, 0.87, 0.9)$ and $(2.490, 0.95, 0.9)$ are suggested in Table 4 of Lu (2015) for detecting various shifts, including small, moderate and large shifts, respectively.

(Please insert Table 6 here)

The simulation results show that the GWMA SN chart is slightly more efficient than the EWMA SN chart in detecting small shifts, but none of them, of course, can perform uniformly better for all shift sizes. However, it is interesting to note that the relative efficiency loss of the CAEWMA SN chart for small (or large) shift sizes is negligible but the relative efficiency gain for large (or small) shift sizes is remarkable. For instance, in Table 6, when compard with the GWMA SN chart with $q = 0.87$, the percentage increase (i.e., $\left|\mathrm{ARL}_1^{\mathrm{AEWMA}} - \mathrm{ARL}_1^{\mathrm{EWMA}}\right| / \mathrm{ARL}_1^{\mathrm{EWMA}} \times 100\%$) in the ARL values of the CAEWMA SN chart for $p_1 = 0.45$ is 7.33% ($|36.6 - 34.1|/34.1$), while the percentage decrease at $p_1 = 0.1$ is 33.30% ($|1.4 - 2.1|/2.1$). The superiority of the CAEWMA SN chart in catching up with a wide range of shifts has also been verified in terms of the RMI performance. For example, the GWMA SN chart with $q = 0.6$ achieves the smallest RMI = 0.11 value among all GWMA designs while, we observe that the RMI value of the CAEWMA SN chart is only 0.08.

Comparisons with the CEWMA SN **chart**

The combinations $(K^*, \gamma_X^*, \gamma_Y^*)$ provided in Table 3 of Castagliola et al. (2018) are optimal in the sense that, among all the possible combinations for $\mathrm{ARL}_0 \approx 370.4$, the noted one gives the smallest ARL_1 value for $p_1 \in \{0.05, 0.1, \ldots, 0.45\}$, respectively. In Table 7, we present the optimal combinations $(K^*, \gamma_X^*, \gamma_Y^*)$ and the ARL values of the CEWMA SN chart for $n = 20$. Due to the discreteness of the parameters, it could exist a combination $(K^*, \gamma_X^*, \gamma_Y^*)$ having the minimum ARL_1 for several shifts. For example, the combination $(9, 7, 4)$ simultaneously provides the minimum ARL_1 for small shifts $p_1 \in \{0.05, 0.1, 0.15\}$, the combination $(8, 1, 1)$ for moderate shifts $p_1 \in \{0.2, 0.25\}$, the combination $(4, 3, 16)$ for large shifts $p_1 \in \{0.35, 0.4\}$, etc.

(Please insert Table 7 here)

The results also show that the CAEWMA SN chart has superior efficiency for detecting a wide range of shifts as we would expect. It can be seen that:

- For small shifts $p_1 \geq 0.35$, the proposed CAEWMA SN chart has a similar performance as for the CEWMA SN chart with $(4, 3, 16)$ and $(2, 4, 87)$, but it is more competitive for large shifts $p_1 \leq 0.2$.
- For moderate shifts $0.15 \leq p_1 < 0.35$, the proposed CAEWMA SN chart has a similar performance as for the CEWMA SN chart with $(7, 7, 11)$, but it is more competitive for large shifts $p_1 < 0.15$ and small shifts $p_1 \geq 0.35$.
- For large shifts $p_1 < 0.15$, the proposed CAEWMA SN chart has a similar performance as for the CEWMA SN chart with $(9, 7, 4)$ and $(8, 1, 1)$, but it is more competitive for small shifts $p_1 \geq 0.35$.

To conclude, from the comparisons in terms of the RMI measure shown in Tables 4 to 7, it is obvious that the CAEWMA SN chart achieves the best performance among all competing designs. This agrees with the expectation of the superiority of AEWMA-type schemes over EMWA-type schemes in catching up with a wide range of shifts. Since the CAEWMA SN chart preserves its property as a more competitive scheme for detecting small and large shifts simultaneously, thus we recommend the implementation of the CAEWMA SN chart if the actual size of the shift is unpredictable in practice.

6 In-control robustness

From a practical standpoint, we further investigate the in-control robustness of the corresponding parametric AEWMA scheme in order to get more insight concerning the benefits of the proposed nonparametric chart. The in-control robustness is the key to the proper design and implementation of any control chart, lack of which can render its out-of-control shift detection capability almost meaningless. Therefore, it is of interest to compare the in-control performance of the CAEWMA SN chart with the parametric AEWMA chart (designed for normality) when the underlying distributional assumption is violated. Our study includes a wide collection of symmetric distributions including the normal and non-normal ones: (i) the standard Normal distribution NOR$(0, 1)$; (ii) the scaled Student's t-distribution, t$(4)/\sqrt{4/4-2}$; (iii) the Laplace distribution (or double exponential) LA$(0, 1/\sqrt{2})$; (iv) the Logistic distribution, LG$(0, \sqrt{3}/\pi)$; (v) the Contaminated Normal (CN) distribution, i.e. a mixture c.d.f. $F_{CN}(x) = (1-\tau)\Phi(x|0,1) + \tau\Phi(x|0,2)$ with a level of contamination $\tau = 0.1$. All the distributions under consideration have have been selected in order to have a mean equal to 0 and a standard deviation equal to 1 (for the CN data, the "dominant" part of the data come from a NOR$(0, 1)$ distribution), so that the results are easily comparable across distributions. The values of the in-control RL characteristics have been estimated via Monte Carlo simulation (50,000 runs) resulting in a standard error is less than 0.1%. The results are shown in Figures 1 and 2 for subgroup size $n = 10$ and 20, respectively.

(Please insert Figures 1 and 2 here)

In each boxplot of Figures 1 and 2, the mean of the run-length distribution is marked with a circle. As the CAEWMA SN chart is a distribution free chart, the first (leftmost) boxplot is the one corresponding to the CAEWMA SN chart independently of the distribution under consideration. The five remaining boxplots correspond to the AEWMA chart for the five distribution under consideration. Also, a reference line was inserted on the vertical axis at 500, which is the desired nominal ARL_0 value in this case.

From Figures 1 and 2, it can be seen that the AEWMA $\bar{X}$ chart is not robust and its in-control run-length distribution is highly affected by a change in the underlying distribution. For example, focussing on ARL_0 as a measure of location, for $n = 20$, the ARL_0 of the AEWMA $\bar{X}$ chart varies from 500.0 (when the underlying distribution is NOR$(0, 1)$) to 314.7 (for t$(4)/\sqrt{4/4-2}$), 428.4 (for LA$(0, 1/\sqrt{2})$, 471.1 (for LG$(0, 1/\sqrt{2})$) and 169.1 (for CN), respectively. In addition, for $n = 10$, the ARL_0 values of the AEWMA $\bar{X}$ chart are much smaller than 500 for all the considered distributions. The consequence will be many more false alarms than it was nominally expected. On the other hand, the CAEWMA SN chart has stable performances for all distributions under consideration, indicating that this nonparametric scheme has a better non-normal robustness and outlier resistance.

7 Two illustrative examples

7.1 Beverage example

The goal of this example is to illustrate the use of the CAEWMA SN chart when the underlying distribution cannot be exactly ascertained. As in Celano et al. (2016) and Castagliola et al. (2018), a soft drink filling process is considered, and the quality characteristic X is the quantity of CO_2 dissolved within the soft drink. In fact, taking account of the thin wall and the high bottling pressure of polyethylene terephthalate (PET) bottles, there is a need for a strict control of the dissolved CO_2 level. For confidentiality reasons, the in-control median value θ_0 can not be explicitly reported here. In Table 8, we report the deviation from target values $X_{t,j} - \theta_0$ of the quantity of dissolved CO_2 for $t = 1, 2, \ldots, 10$ periods and $j = 1, 2, \ldots, 7$ corresponding to a Phase II implementation.

The practitioner decided to use control charts designed for detecting a shift of $p_{\text{opt}} = 0.4$ based on $\text{ARL}_0 = 370.4$. The optimal set of parameters of the CAEWMA SN chart are found to be $(h^*, \gamma_X^*, \gamma_Y^*, k^*) = (5, 1, 6, 3)$ and the competing optimal CEWMA SN chart $(h^*, \gamma_X^*, \gamma_Y^*, k^*) = (3, 2, 7)$ recommended in Castagliola et al. (2018) is also constructed. Normality has been tested and not rejected for observations from the measurement system, but the in-control σ_0 is unknown. Therefore, the parametric AEWMA $\bar{X}$ chart $(h^*, \lambda^*, k^*) = (0.811, 0.15, 3.25)$ is also constructed and we use the the sample standard variance $\bar{S}_V = \frac{1}{10}\sum_{t=1}^{10} S_{V,t}$ to estimate the σ_0, where $\bar{V}_t = \frac{1}{n}\sum_{k=1}^{n} V_{t,k}$ and $S_{V,t} = \sqrt{\frac{1}{n-1}\sum_{k=1}^{n}(V_{t,k} - \bar{V}_t)}$.

The monitoring statistics of the parametric AEWMA $\bar{X}$ chart, the CAEWMA SN chart and the CEWMA SN chart are thus plotted against their control limits, in Figure 3. It can be seen that the AEWMA chart does not show any out-of-control signal in the process location. The CAEWMA SN chart signals at the 5^{th} observation followed by the CEWMA SN chart at 6^{th}, suggesting an upward shift in the process median (i.e. more CO_2 dissolved in each bottle). The parametric AEWMA $\bar{X}$ chart signals at 7^{th}. This performance difference can be explained by the presence of the "noise" observations in the samples (in Celano et al. (2016), it was proved that the observations are from a mixture of two normal distributions.), which increases the value of the sample standard deviation, thus reducing the sensitivity of the parametric AEWMA $\bar{X}$ chart to a shift in the process mean.

This is not surprising, as in practice, normality can be often in doubt or may not be justified because of lack of information or data, and the proposed CAEWMA SN chart offers an effective alternative over available parametric and nonparametric control charts.

(Please insert Table 8 and Figure 1 here)

7.2 Manufacturing example

The goal of this example is to illustrate the superiority of the CAEWMA SN chart for detecting a range of shifts Ω_{opt}. For the sake of comparison, the competing CEWMA SN chart is also constructed. The data-set is taken from a printed circuit manufacturing industry. The quality level of their products is monitored with subgroups of size $n = 12$ and it consists of 30×12 observations from a normal distribution with an in-control mean/median $\theta_0 = 50$ and an in-control standard deviation $\sigma_0 = 1.0$. We consider two different out-of-control situations, one for detecting $0.5 \times \sigma_0$ (a small shift $p_1 \approx 0.31$) and one for detecting $1.5 \times \sigma_0$ (a large shift $p_1 \approx 0.07$) in the last 20 observations. The desired ARL_0 value is fixed at 370.4. Based on Table 3 of Castagliola et al. (2018), the optimal combinations $(K^*, \gamma_X^*, \gamma_Y^*) = (7, 7, 5)$ and (3,3,19) of CEWMA SN charts (denoted as CEWMA-1 and CEWMA-2) designed for $p_{\text{opt}} = 0.05$ and 0.3, respectively, are considered here. Concerning the

CAEWMA SN chart, based on the searching procedure in Section 5.2, the optimal combination is obtained to be $(h^*, \gamma_X^*, \gamma_Y^*, k^*) = (4, 2, 7, 9)$.

The data of the deviation from target values $X_{t,j} - \theta_0$ and the statistics SN_t, together with statistics Y_t and R_t of the CEWMA-1, the CEWMA-2 and the CAEWMA charts, are shown in Tables 9 and 10. When the process is in-control (i.e. the first $t = 1, 2, \ldots, 10$ observations), we can observe that the three charts are all in an in-control state. In Table 9, for the small shift $p_1 \approx 0.31$ case, both the CEWMA-2 and the CAEWMA charts signal at the 18^{th} observation and the CEWMA-1 chart signals at the 24^{th} observation. While, for the large shift $p_1 \approx 0.07$ case in Table 10, the CAEWMA chart signals at the 10^{th} observation followed by the CEWMA-1 chart at 11^{th} and the CEWMA-2 chart at 12^{th}. Note that the CAEWMA chart is not only as effective as the CEWMA-2 chart when the shift is small, but it is also more effective for large shifts than the two CEWMA charts. Therefore, We can conclude that the CAEWMA scheme is more sensitive to various shifts than the CEWMA scheme in this example. In Figures 2 and 3, we also have plotted the three charts corresponding to the data in Tables 9 and 10, respectively.

(Please insert Tables 9 and 10, and Figures 2 and 3 here)

8 Conclusions

In this paper, we propose a new nonparametric CAEWMA SN chart with exact run length properties, which combines the advantages of a nonparametric control chart with the better overall shift detection properties of the AEWMA scheme. An in-depth study to gain insight into its design, implementation and performance has been done. More precisely: i) An appropriate discrete time Markov-chain technique is presented to calculate the exact run length distribution and the associated performance characteristics without expensive simulations or unreliable approximations; ii) To aid practical implementation, some optimal parameters are presented and for a more thorough assessment of the chart's performance, we also calculate the RMI for an overall assessment when a range of shifts are considered; iii) We propose two optimal designs based on the ARL and the AARL as performance measures, respectively. A simulation study demonstrates that the proposed control chart not only performs robustly for different distributions, but also is efficient in detecting various magnitude of shifts.

A possible topic for further research would be to extend a modified version, a CAEWMA Wilcoxon signed-rank chart, which probably provides a better efficiency for monitoring observations of symmetric distributions. Moreover, adaptations to the case for monitoring the process dispersion (scale) when the distribution of observations is unknown, would also be a very challenging issue to be investigated as an extension of this research.

Disclosure statement

No potential conflict of interest was reported by the authors.

Appendix 1

Algorithm Computation of transient probabilities $q_{i,j}$

Define n, p, h, γ_X, γ_Y and k
$c \leftarrow h(\gamma_X + \gamma_Y) - 1$
For $i = -c, -c+1, \ldots, c$
  For $\mathrm{SN}_t = -n, -n+2, \ldots, n-2, n$
    $y_{t-1} \leftarrow \left\lfloor \frac{i}{\gamma_X+\gamma_Y} \right\rfloor$
    $e_t \leftarrow \mathrm{SN}_t - y_{t-1}$
    If $e_t < -k$
      $\varphi(e_t) \leftarrow e_t(\gamma_X + \gamma_Y) + k\gamma_Y$
    Else if $e_t > k$
      $\varphi(e_t) \leftarrow e_t(\gamma_X + \gamma_Y) - k\gamma_Y$
    Else $-k \le e_t \le k$
      $\varphi(e_t) \leftarrow e_t\gamma_X$
    End If
    $y_t \leftarrow \left\lfloor \frac{\varphi(e_t)+i}{\gamma_X+\gamma_Y} \right\rfloor$
    If $-h < y_t < h$ **Then**
      $r_t \leftarrow \varphi(e_t) + i - (\gamma_X + \gamma_Y)y_t$
      $j \leftarrow (\gamma_X + \gamma_Y)y_t + r_t$
      $q_{i,j} \leftarrow f_B(\frac{\mathrm{SN}_t+n}{2}|n, p)$
    End If
  End For
End For

Appendix 2

The following Algorithm is used in Section 5 to find the optimal combination $(h^*, \gamma_X^*, \gamma_Y^*, k^*)$:

Algorithm For detecting a specific magnitude of the shift p_{opt}

Define n, $p_0 = 0.5$, $p_{\text{opt}} \in (0, 0.5)$
$\text{ARL}_0 \leftarrow 370.4$
$\text{ARL}^* \leftarrow \infty$
For $h = 1, 2, \ldots, n$
  For $k = 1, 2, \ldots, n$
    For $\gamma_X = 1, 2, \ldots, 10$
      $\gamma_Y \leftarrow 0$
      Repeat
      $\gamma_Y \leftarrow \gamma_Y + 1$
      Until $\left|\frac{\text{ARL}(h,\gamma_X,\gamma_Y,k,n,p_0)-\text{ARL}_0}{\text{ARL}_0}\right| \leq 0.05$
      If $\text{ARL}(h, \gamma_X, \gamma_Y, k, n, p_{\text{opt}}) < \text{ARL}^*$ **Then**
        $\text{ARL}^* \leftarrow \text{ARL}(h, \gamma_X, \gamma_Y, k, n, p_{opt})$
        $h^* \leftarrow h$,$\gamma_X^* \leftarrow \gamma_X$,$\gamma_Y^* \leftarrow \gamma_Y$ and $k^* \leftarrow k$
      End If
    End For
  End For
End For

Algorithm For detecting a range of unknown shifts Ω_{opt}

Define n, $p_0 = 0.5$, $\Omega_{\text{opt}} = \{0.05, 0.1, \ldots, 0.45\}$
$\text{ARL}_0 \leftarrow 370.4$
$\text{AARL}^* \leftarrow \infty$
For $h = 1, 2, \ldots, n$
  For $k = 1, 2, \ldots, n$
    For $\gamma_X = 1, 2, \ldots, 10$
      $\gamma_Y \leftarrow 0$
      Repeat
      $\gamma_Y \leftarrow \gamma_Y + 1$
      Until $\left|\frac{\text{ARL}(h,\gamma_X,\gamma_Y,k,n,p_0)-\text{ARL}_0}{\text{ARL}_0}\right| \leq 0.05$
      $\text{AARL} \leftarrow 0$
      For $p_1 = 0.05, 0.1, \ldots, 0.45$
        $\text{AARL} \leftarrow \text{AARL} + \omega_{p_1} \times \text{ARL}(h, \gamma_X, \gamma_Y, k, n, p_1)$
      End For
      If $\text{AARL}(h, \gamma_X, \gamma_Y, k, n, \Omega_{\text{opt}}) < \text{AARL}^*$ **Then**
        $\text{AARL}^* \leftarrow \text{AARL}(h, \gamma_X, \gamma_Y, k, n, \Omega_{\text{opt}})$
        $h^* \leftarrow h$,$\gamma_X^* \leftarrow \gamma_X$,$\gamma_Y^* \leftarrow \gamma_Y$ and $k^* \leftarrow k$
      End If
    End For
  End For
End For

References

Abid M, Nazir HZ, Riaz M and Lin Z. 2017. "An efficient nonparametric EWMA Wilcoxon signed-rank chart for monitoring location." *Quality and Reliability Engineering International* 33(3):669–685.

Albers W and Kallenberg WC. 2004. "Empirical non-parametric control charts: estimation effects and corrections." *Journal of applied statistics* 31(3):345–360.

Aly AA, Hamed RM and Mahmoud MA. 2017. "Optimal design of the adaptive exponentially weighted moving average control chart over a range of mean shifts." *Communications in Statistics-Simulation and Computation* 46(2):890–902.

Aly AA, Saleh NA, Mahmoud MA and Woodall WH. 2015. "A reevaluation of the adaptive exponentially weighted moving average control chart when parameters are estimated." *Quality and Reliability Engineering International* 31(8):1611–1622.

Aslam M, Azam M and Jun CH. 2014. "A new exponentially weighted moving average sign chart using repetitive sampling." *Journal of Process Control* 24(7):1149-1153.

Bakir ST. 2004. "A distribution-free Shewhart quality control chart based on signed-ranks." *Quality Engineering* 16(4):613–623.

Capizzi G and Masarotto G. 2003. "An adaptive exponentially weighted moving average control chart." *Technometrics* 45(3):199–207.

Castagliola P, Tran KP, Celano G, Rakitzis AC and Maravelakis PE. 2018. (forthcoming) "An EWMA-Type Sign Chart with Exact Run Length Properties." *Journal of Quality Technology*

Celano G, Castagliola P, Chakraborti S and Nenes G. 2016. "The performance of the Shewhart sign control chart for finite horizon processes." *The International Journal of Advanced Manufacturing Technology* 84(5):1497–1512.

Chakraborti S and Eryilmaz S. 2007. "A nonparametric Shewhart-type signed-rank control chart based on runs." *Communications in Statistics-Simulation and Computation* 36(2):335–356.

Chakraborti S, Human SW and Graham MA. 2011. "Nonparametric (distribution-free) quality control charts." In N. Balakrishnan, editor, *Handbook of Methods and Applications of Statistics: Engineering, Quality Control, and Physical Sciences*, pages 298–329. John Wiley & Sons, 2011.

Chakraborti S, Qiu P and Mukherjee A. 2015. "Editorial to the special issue: Nonparametric statistical process control charts." *Quality and Reliability Engineering International* 31(1):1–2.

Chakraborty N, Chakraborti S, Human SW and Balakrishnan N. 2016. "A generally weighted moving average signed-rank control chart." *Quality and Reliability Engineering International* 32(8):2835–2845.

Gibbons JD and Chakraborti S. *Nonparametric statistical inference.* Chapman and Hall/CRC, 2010.

Graham MA, Chakraborti S and Human SW. 2011. "A nonparametric exponentially weighted moving average signed-rank chart for monitoring location." *Computational Statistics & Data Analysis* 55 (8):2490–2503.

Graham MA, Mukherjee A and Chakraborti S . 2012. "Distribution-free exponentially weighted moving average control charts for monitoring unknown location." *Computational Statistics & Data Analysis* 56(8):2539-2561.

Graham MA, Mukherjee A and Chakraborti S . 2017. "Design and implementation issues for a class of distribution-free Phase II EWMA exceedance control charts." *International Journal of Production Research* 55(8):2397-2430.

Han D and Tsung F. 2006. "A reference-free cuscore chart for dynamic mean change detection and a unified framework for charting performance comparison." *Journal of the American Statistical Association* 101(473):368–386.

Haq A and Khoo MB. 2018. "A new non-parametric multivariate EWMA sign control chart for monitoring process dispersion." *Communications in Statistics-Theory and Methods* DOI:10.1080/03610926.2018.1476708.

Human SW, Chakraborti S and Smit CF. 2010. "Nonparametric Shewhart-type sign control charts based on runs." *Communications in Statistics-Theory and Methods* 39(11):2046–2062.

Jones-Farmer LA, Jordan V and Champ CW. 2009. "Distribution-free phase I control charts for subgroup location." *Journal of Quality Technology* 41(3):304–316.

Li SY, Tang LC and Ng SH. 2010. "Nonparametric CUSUM and EWMA control charts for detecting mean shifts." *Journal of Quality Technology* 42(2):209–226.

Lu SL. 2015. "An extended nonparametric exponentially weighted moving average sign control chart." *Quality and Reliability Engineering International* 31(1):3–13.

Mukherjee A and Marozzi M. 2017. "Distribution-free Lepage Type Circular-grid Charts for Joint Monitoring of Location and Scale Parameters of a Process." *Quality and Reliability Engineering International* 33(2):241–274.

Noorossana R, Fathizadan S and Nayebpour MR. 2016. "EWMA control chart performance with estimated parameters under no-normality." *Quality and Reliability Engineering International* 32 (5):1637-1654.

Ou Y, Wu Z and Tsung F. 2012. "A comparison study of effectiveness and robustness of control charts for monitoring process mean." *International journal of production economics* 135(1):479–490.

Rakitzis AC, Castagliola P and Maravelakis PE. 2015. "A new memory-type monitoring technique for count data." *Computers & Industrial Engineering* 85:235–247.

Saleh NA, Mahmoud MA and Abdel-Salam ASG. 2013. "The performance of the adaptive exponentially weighted moving average control chart with estimated parameters." *Quality and Reliability Engineering International* 29(4):595–606.

Saleh N, Mahmoud M, Jones-Farmer L, Zwetsloot I and Woodall W. 2015. "Another look at the EWMA control charts with estimated parameters." *Journal of Qualtiy Technology* 47(4):363–382.

Tang A, Castagliola P, Sun J and Hu X. 2017. "An adaptive exponentially weighted moving average chart for the mean with variable sampling intervals." *Quality and Reliability Engineering International* 33(8):2023–2034.

Tang A, Castagliola P, Sun J and Hu X. 2018a. "The effect of measurement errors on the adaptive EWMA $\bar{X}$ chart." *Quality and Reliability Engineering International* DOI:10.1002/qre.2275.

Tang A, Castagliola P, Sun J and Hu X. 2018b. "Optimal design of the adaptive EWMA chart for the mean based on median run length and expected median run length." *Quality Technology & Quantitative Management* DOI:10.1080/16843703.2018.1460908.

Triantafyllou IS. 2018. "Nonparametric control charts based on order statistics: Some advances." *Communications in Statistics-Simulation and Computation* 47(9):2684–2702.

Weiß CH. 2009. "EWMA monitoring of correlated processes of Poisson counts." *Quality Technology & Quantitative Management* 6(2):137–153.

Yang SF, Lin JS and Cheng SW. 2011. "A new nonparametric EWMA sign control chart." *Expert Systems with Applications* 38(5):6239–6243.

Zhou C, Zou C, Zhang Y and Wang Z. 2009. "Nonparametric control chart based on change-point model." *Statistical Papers* 50(1):13–28.

Zi X, Zou C, Zhou Q and Wang J. 2013. "A directional multivariate sign EWMA control chart." *Quality Technology & Quantitative Management* 10(1):115–132.

Zou C. and Tsung F. 2010. "Likelihood ratio-based distribution-free EWMA control charts." *Journal of Quality Technology* 42(2):174–196.

Zou C. and Tsung F. 2011. "A multivariate sign EWMA control chart." *Technometrics* 53(1):84–97.

Table 1: Structure of the matrix $\mathbf{Q}$ for the case $n = 10$, $h = 3$, $\gamma_X = 1$, $\gamma_Y = 3$ and $k = 5$

i \ j	-11	-10	-9	-8	-7	-6	-5	-4	-3	-2	-1	0	1	2	3	4	5	6	7	8	9	10	11
-11	-2	.	0	.	2	.	4	.	6	.	8	.	.	.	.	.	.	.	10	.	.	.	.
-10	.	-2	.	0	.	2	.	4	.	6	.	8	.	.	.	.	.	.	.	10	.	.	.
-9	-4	.	-2	.	0	.	2	.	4	.	6	.	8	.	.	.	.	.	.	.	10	.	.
-8	.	-4	.	-2	.	0	.	2	.	4	.	6	.	8	.	.	.	.	.	.	.	10	.
-7	.	-4	.	-2	.	0	.	2	.	4	.	6	.	8	.	.	.	.	10	.	.	.	.
-6	-6	.	-4	.	-2	.	0	.	2	.	4	.	6	.	8	.	.	.	.	10	.	.	.
-5	.	-6	.	-4	.	-2	.	0	.	2	.	4	.	6	.	8	.	.	.	.	10	.	.
-4	-8	.	-6	.	-4	.	-2	.	0	.	2	.	4	.	6	.	8	.	.	.	.	10	.
-3	-8	.	-6	.	-4	.	-2	.	0	.	2	.	4	.	6	.	8	.	10	.	.	.	.
-2	.	-8	.	-6	.	-4	.	-2	.	0	.	2	.	4	.	6	.	8	.	10	.	.	.
-1	-10	.	-8	.	-6	.	-4	.	-2	.	0	.	2	.	4	.	6	.	8	.	10	.	.
0	.	-10	.	-8	.	-6	.	-4	.	-2	.	0	.	2	.	4	.	6	.	8	.	10	.
1	.	.	-10	.	-8	.	-6	.	-4	.	-2	.	0	.	2	.	4	.	6	.	8	.	10
2	.	.	.	-10	.	-8	.	-6	.	-4	.	-2	.	0	.	2	.	4	.	6	.	8	.
3	.	.	.	.	-10	.	-8	.	-6	.	-4	.	-2	.	0	.	2	.	4	.	6	.	8
4	.	-10	.	.	.	.	-8	.	-6	.	-4	.	-2	.	0	.	2	.	4	.	6	.	8
5	.	.	-10	.	.	.	.	-8	.	-6	.	-4	.	-2	.	0	.	2	.	4	.	6	.
6	.	.	.	-10	.	.	.	.	-8	.	-6	.	-4	.	-2	.	0	.	2	.	4	.	6
7	.	.	.	.	-10	.	.	.	.	-8	.	-6	.	-4	.	-2	.	0	.	2	.	4	.
8	.	-10	.	.	.	.	.	.	.	-8	.	-6	.	-4	.	-2	.	0	.	2	.	4	.
9	.	.	-10	.	.	.	.	.	.	.	-8	.	-6	.	-4	.	-2	.	0	.	2	.	4
10	.	.	.	-10	.	.	.	.	.	.	.	-8	.	-6	.	-4	.	-2	.	0	.	2	.
11	.	.	.	.	-10	.	.	.	.	.	.	.	-8	.	-6	.	-4	.	-2	.	0	.	2

Table 2: Optimal combinations $(h^*, \gamma_X^*, \gamma_Y^*, k^*)$ (first line of each block) and the out-of-control (ARL, SDRL) (second line) for the CAEWMA SN chart along with the corresponding out-of-control (ARL, SDRL) (third line) for the CEWMA SN chart based a specific magnitude of the shift $p_{\text{opt}} \in \{0.05, 0.1, \ldots, 0.45\}$

Type	p_{opt}								
	0.05	0.10	0.15	0.20	0.25	0.30	0.35	0.40	0.45
					$n = 10$				
CAEWMA	(7,9,5,6)	(7,9,5,6)	(5,9,16,7)	(5,9,16,7)	(5,9,14,9)	(4,5,13,10)	(4,5,13,10)	(2,9,113,10)	(2,9,113,10)
	(1.4,0.6)	(1.9,0.9)	(2.6,1.2)	(3.5,1.7)	(4.7,2.3)	(6.8,3.4)	(11.3,7.2)	(20.1,9.6)	(53.2,37.3)
CEWMA	(2.2,0.4)	(2.6,0.6)	(3.1,0.8)	(3.7,1.2)	(4.8,1.9)	(6.8,3.4)	(11.3,7.2)	(24.8,20.2)	(61.1,24.6)
					$n = 11$				
CAEWMA	(6,1,1,10)	(6,1,1,10)	(6,1,1,10)	(6,1,1,10)	(5,9,16,9)	(4,5,15,11)	(4,8,24,11)	(4,5,15,11)	(2,1,14,10)
	(1.4,0.5)	(1.8,0.7)	(2.3,1.0)	(3.1,1.6)	(4.3,2.0)	(6.1,2.9)	(9.9,6.0)	(21.3,16.5)	(49.2,33.8)
CEWMA	(2.1,0.3)	(2.4,0.5)	(2.8,0.8)	(3.5,1.1)	(4.4,1.7)	(6.1,2.9)	(9.9,6.0)	(21.3,16.5)	(57.9,22.8)
					$n = 12$				
CAEWMA	(6,6,7,10)	(6,6,7,10)	(6,6,7,10)	(6,6,7,10)	(6,6,7,10)	(4,7,24,9)	(4,7,24,9)	(3,7,44,11)	(2,2,30,11)
	(1.5,0.5)	(1.8,0.6)	(2.3,0.8)	(2.9,1.3)	(4.0,2.1)	(5.8,2.6)	(9.2,5.3)	(16.8,10.0)	(45.4,29.7)
CEWMA	(1.5,0.5)	(1.8,0.6)	(2.3,0.9)	(3.1,1.5)	(4.5,2.8)	(6.4,2.2)	(9.3,4.1)	(16.9,10.0)	(45.8,29.8)
					$n = 13$				
CAEWMA	(9,9,2,10)	(9,9,2,10)	(9,9,2,12)	(9,9,2,12)	(5,5,11,10)	(5,5,11,10)	(4,10,37,10)	(3,10,67,11)	(2,7,109,11)
	(1.1,0.4)	(1.4,0.6)	(1.9,1.0)	(2.8,1.7)	(3.7,1.6)	(5.3,2.7)	(8.4,4.4)	(16.2,9.2)	(43.5,27.7)
CEWMA	(1.1,0.4)	(1.4,0.6)	(1.9,1.0)	(2.8,1.8)	(3.9,1.8)	(5.5,2.4)	(8.5,4.4)	(16.9,11.6)	(53.8,20.2)
					$n = 14$				
CAEWMA	(8,8,5,8)	(8,8,5,8)	(8,8,5,8)	(8,8,5,8)	(6,7,11,9)	(5,7,16,11)	(4,2,8,11)	(3,3,23,11)	(2,7,116,12)
	(1.2,0.4)	(1.5,0.6)	(1.9,0.9)	(2.6,1.4)	(3.7,1.9)	(5.3,2.5)	(8.1,4.2)	(15.1,8.2)	(41.0,25.0)
CEWMA	(1.2,0.4)	(1.5,0.7)	(2.0,1.1)	(2.9,1.8)	(4.6,3.4)	(8.2,6.9)	(17.2,3.5)	(25.7,6.6)	(51.1,19.0)
					$n = 15$				
CAEWMA	(8,5,3,13)	(7,5,5,12)	(7,1,1,12)	(7,3,3,12)	(6,8,13,11)	(5,9,23,11)	(4,7,29,12)	(3,2,15,13)	(2,1,18,12)
	(1.2,0.4)	(1.5,0.6)	(1.9,0.8)	(2.4,1.1)	(3.4,1.5)	(4.8,2.2)	(7.6,3.7)	(14.2,7.4)	(39.1,23.5)
CEWMA	(2.0,0.1)	(2.1,0.3)	(2.3,0.5)	(2.8,0.8)	(3.5,1.3)	(4.9,2.2)	(7.7,3.7)	(14.2,7.2)	(42.4,32.5)
					$n = 16$				
CAEWMA	(8,7,9,7)	(8,7,9,7)	(8,7,9,7)	(7,7,8,11)	(7,7,8,11)	(5,9,25,11)	(4,2,9,13)	(3,1,8,15)	(2,5,93,13)
	(1.0,0.2)	(1.3,0.5)	(1.7,0.9)	(2.4,0.9)	(3.2,1.5)	(4.7,2.1)	(7.3,3.3)	(13.4,6.8)	(37.5,21.6)
CEWMA	(1.0,0.2)	(1.2,0.5)	(1.6,0.8)	(2.2,1.4)	(3.5,2.6)	(4.8,2.0)	(7.3,3.3)	(13.4,6.8)	(39.2,29.4)
					$n = 17$				
CAEWMA	(8,8,9,8)	(8,10,11,8)	(8,10,11,8)	(8,8,7,10)	(8,8,7,10)	(5,3,8,16)	(5,3,8,16)	(4,5,23,14)	(2,3,58,15)
	(1.1,0.2)	(1.3,0.5)	(1.6,0.7)	(2.2,1.1)	(3.1,1.7)	(4.5,1.9)	(7.0,3.7)	(13.0,7.9)	(35.2,19.6)
CEWMA	(1.2,0.4)	(1.5,0.5)	(1.9,0.6)	(2.4,1.0)	(3.3,1.7)	(4.5,1.9)	(7.0,3.7)	(13.1,7.9)	(35.2,19.6)
					$n = 18$				
CAEWMA	(9,9,5,14)	(9,9,5,14)	(8,7,6,13)	(8,7,6,13)	(8,7,6,13)	(6,6,13,11)	(5,3,9,16)	(4,8,40,14)	(2,1,20,17)
	(1.1,0.2)	(1.3,0.5)	(1.6,0.7)	(2.1,0.9)	(3.0,1.5)	(4.2,2.1)	(6.6,3.4)	(12.5,7.2)	(33.6,18.3)
CEWMA	(1.2,0.4)	(1.6,0.5)	(1.9,0.6)	(2.3,0.8)	(3.0,1.3)	(4.3,1.9)	(6.6,3.4)	(12.5,5.8)	(33.6,18.3)
					$n = 19$				
CAEWMA	(8,7,17,7)	(8,7,17,7)	(8,7,17,7)	(8,7,17,7)	(7,7,10,13)	(7,7,10,13)	(5,8,27,12)	(4,5,27,13)	(2,1,21,15)
	(1.0,0.1)	(1.1,0.4)	(1.4,0.7)	(2.1,1.3)	(2.8,1.2)	(4.0,2.0)	(6.3,3.2)	(12.1,6.7)	(32.8,17.5)
CEWMA	(1.1,0.2)	(1.3,0.5)	(1.6,0.6)	(2.1,0.9)	(2.9,1.5)	(4.1,1.8)	(6.5,3.8)	(12.2,5.4)	(32.8,17.5)
					$n = 20$				
CAEWMA	(8,7,8,11)	(8,7,8,11)	(8,7,8,11)	(8,7,8,11)	(8,7,8,11)	(6,7,16,13)	(5,4,13,15)	(4,3,16,16)	(2,3,66,16)
	(1.0,0.1)	(1.1,0.4)	(1.4,0.6)	(1.9,0.9)	(2.7,1.5)	(3.9,1.7)	(6.2,3.0)	(11.4,6.2)	(32.0,16.6)
CEWMA	(1.1,0.3)	(1.3,0.5)	(1.7,0.6)	(2.1,0.8)	(2.8,1.2)	(4.0,1.9)	(6.4,2.5)	(11.4,6.2)	(32.0,16.6)
					$n = 21$				
CAEWMA	(8,4,5,11)	(8,9,11,11)	(8,9,11,11)	(8,9,11,11)	(8,8,9,13)	(7,10,17,12)	(6,4,9,18)	(4,5,28,16)	(3,7,74,15)
	(1.0,0.1)	(1.2,0.4)	(1.4,0.6)	(1.9,0.8)	(2.5,1.2)	(3.8,1.9)	(5.9,3.2)	(11.0,5.8)	(31.0,20.1)
CEWMA	(1.0,0.1)	(1.2,0.4)	(1.4,0.6)	(1.9,0.9)	(2.7,1.5)	(3.8,1.8)	(5.9,3.2)	(11.0,5.8)	(31.1,20.1)
					$n = 22$				
CAEWMA	(12,9,1,21)	(12,9,1,21)	(12,9,1,22)	(12,9,1,22)	(8,9,11,13)	(7,7,13,12)	(6,9,22,15)	(4,1,6,17)	(3,2,21,17)
	(1.0,0.1)	(1.1,0.3)	(1.3,0.5)	(1.7,1.0)	(2.5,1.1)	(3.6,1.7)	(5.7,2.9)	(10.5,5.3)	(29.4,19.0)
CEWMA	(1.0,0.1)	(1.1,0.3)	(1.3,0.5)	(1.7,1.0)	(2.7,1.9)	(3.7,1.6)	(5.7,2.8)	(10.5,5.3)	(29.5,19.0)
					$n = 23$				
CAEWMA	(10,6,4,12)	(10,9,6,12)	(10,9,6,12)	(10,9,6,12)	(8,5,7,12)	(8,4,5,16)	(6,3,8,14)	(4,8,51,15)	(3,4,45,16)
	(1.0,0.1)	(1.1,0.3)	(1.3,0.5)	(1.7,0.8)	(2.4,1.1)	(3.4,1.7)	(5.5,2.7)	(10.5,5.2)	(28.4,17.7)
CEWMA	(1.0,0.1)	(1.1,0.3)	(1.3,0.5)	(1.7,0.9)	(2.4,1.1)	(3.6,2.0)	(5.6,2.7)	(11.0,4.4)	(28.5,17.7)
					$n = 24$				
CAEWMA	(9,8,9,11)	(9,8,9,11)	(9,8,9,11)	(10,10,7,13)	(10,10,7,13)	(8,8,11,14)	(6,6,17,15)	(5,2,8,18)	(3,10,116,19)
	(1.0,0.1)	(1.1,0.3)	(1.3,0.5)	(1.7,0.7)	(2.3,1.2)	(3.4,1.6)	(5.3,2.5)	(10.0,5.7)	(27.2,16.6)
CEWMA	(1.0,0.1)	(1.1,0.3)	(1.3,0.5)	(1.7,0.8)	(2.4,1.3)	(3.5,1.5)	(5.4,2.5)	(10.0,5.7)	(27.2,16.6)
					$n = 25$				
CAEWMA	(10,4,5,9)	(10,4,5,9)	(10,4,5,9)	(10,4,5,9)	(9,1,1,16)	(8,6,9,13)	(6,7,19,18)	(5,5,22,16)	(3,2,24,17)
	(1.0,0.0)	(1.0,0.2)	(1.2,0.4)	(1.5,0.8)	(2.2,1.0)	(3.3,1.6)	(5.2,2.4)	(9.6,5.2)	(26.7,16.1)
CEWMA	(1.0,0.0)	(1.0,0.2)	(1.2,0.4)	(1.6,0.8)	(2.3,1.1)	(3.3,1.5)	(5.2,2.4)	(9.7,5.2)	(26.8,16.1)

Table 3: Some optimal CAEWMA SN charts based on a whole range of shifts $\Omega_{\text{opt}} \sim \{0.05, 0.10, \ldots, 0.45\}$

n	h^*	γ_X^*	γ_Y^*	k^*	n	h^*	γ_X^*	γ_Y^*	k^*
10	3	1	6	8	18	3	10	97	12
11	3	7	43	9	19	3	1	10	13
12	4	2	7	9	20	4	4	23	14
13	3	7	50	10	21	3	3	35	13
14	3	10	81	10	22	4	7	43	15
15	3	4	33	11	23	4	8	51	15
16	3	6	53	11	24	4	4	27	16
17	3	5	51	11	25	4	8	59	14

Table 4: Comparisons of Standard EWMA SN and CAEWMA SN charts when $n = 20$, $p_0 = 0.50$ and $\text{ARL}_0 \approx 370.4$

p	EWMA-S(k^*, λ^*)					CAEWMA$(h^*, \gamma_X^*, \gamma_Y^*, k^*)$
	$(2.49, 0.05)$	$(2.77, 0.15)$	$(2.89, 0.3)$	$(2.93, 0.6)$	$(2.89, 0.9)$	(4,4,23,14)
0.50	376.0	352.5	364.2	364.9	373.6	373.7
0.45	31.1	38.1	57.2	103.1	173.4	36.6
0.40	12.3	11.2	13.5	24.1	51.5	11.5
0.35	7.6	6.2	6.2	8.7	17.3	6.5
0.30	5.6	4.3	3.9	4.4	7.0	4.5
0.25	4.4	3.3	2.9	2.8	3.5	3.3
0.20	3.7	2.7	2.3	2.1	2.1	2.6
0.15	3.2	2.3	2.0	1.4	1.4	2.0
0.10	2.9	2.1	1.9	1.1	1.1	1.4
0.05	2.6	2.0	1.6	1.0	1.0	1.1
RMI	0.33	0.17	0.15	0.20	0.55	0.08

Table 5: Comparisons of Arcsine EWMA SN and CAEWMA SN charts when $n = 20$, $p_0 = 0.50$ and $\text{ARL}_0 \approx 370.4$

p	EWMA-A(k^*, λ^*)					CAEWMA$(h^*, \gamma_X^*, \gamma_Y^*, k^*)$
	$(2.491, 0.05)$	$(2.801, 0.15)$	$(2.925, 0.3)$	$(2.989, 0.6)$	$(3.00, 0.9)$	(4,4,23,14)
0.50	370.4	370.5	370.2	372.0	370.9	373.7
0.45	31.0	38.9	57.8	104.5	158.4	36.6
0.40	12.2	11.3	13.5	24.2	45.4	11.5
0.35	7.5	6.1	6.1	8.6	15.5	6.5
0.30	5.4	4.2	3.8	4.3	6.6	4.5
0.25	4.2	3.2	2.8	2.7	3.4	3.3
0.20	3.5	2.6	2.2	1.9	2.0	2.6
0.15	2.9	2.2	1.8	1.5	1.4	2.0
0.10	2.5	1.9	1.5	1.2	1.1	1.4
0.05	2.1	1.6	1.2	1.0	1.0	1.1
RMI	0.28	0.14	0.11	0.21	0.49	0.09

Table 6: Comparisons of GWMA SN and CAEWMA SN charts when $n = 20$, $p_0 = 0.50$ and $\text{ARL}_0 \approx 370.4$

p	GWMA(L^*, q^*, α^*)				CAEWMA$(h^*, \gamma_X^*, \gamma_Y^*, k^*)$
	$(2.929, 0.4, 0.6)$	$(2.925, 0.6, 0.9)$	$(2.771, 0.87, 0.9)$	$(2.490, 0.95, 0.9)$	(4,4,23,14)
0.50	373.5	370.9	373.5	374.1	373.7
0.45	94.2	67.3	34.1	30.6	36.6
0.40	22.6	15.5	11.1	12.8	11.5
0.35	9.0	6.6	6.5	7.7	6.5
0.30	4.5	3.9	4.5	5.6	4.5
0.25	2.8	2.7	3.5	4.3	3.3
0.20	1.9	2.1	2.8	3.5	2.6
0.15	1.4	1.7	2.4	3.1	2.0
0.10	1.2	1.3	2.1	2.7	1.4
0.05	1.0	1.1	2.0	2.2	1.1
RMI	0.18	0.11	0.18	0.29	0.08

Table 7: Comparisons of CEWMA SN and CAEWMA SN charts when $n = 20$, $p_0 = 0.50$ and $\text{ARL}_0 \approx 370.4$

p	CEWMA$(K^*, \gamma_X^*, \gamma_Y^*)$					CAEWMA$(h^*, \gamma_X^*, \gamma_Y^*, k^*)$
	$(9, 7, 4)$	$(8, 1, 1)$	$(7, 7, 11)$	$(4, 3, 16)$	$(2, 4, 87)$	(4,4,23,14)
0.50	358.5	370.4	384.2	370.2	370.2	373.7
0.45	101.5	84.4	66.5	37.3	37.3	36.6
0.40	24.3	19.2	15.3	11.4	11.4	11.5
0.35	8.9	7.5	6.6	6.4	6.4	6.5
0.30	4.5	4.1	4.0	4.5	4.5	4.5
0.25	2.9	2.8	2.9	3.5	3.5	3.3
0.20	2.1	2.1	2.3	2.9	2.9	2.6
0.15	1.7	1.7	1.9	2.4	2.4	2.0
0.10	1.3	1.3	1.6	2.1	2.1	1.4
0.05	1.1	1.1	1.3	2.0	2.0	1.1
RMI	0.17	0.11	0.09	0.13	0.13	0.04

Table 8: Phase II sample of the beverage example

t	$V_{t,k} = X_{t,k} - \theta_0$							$\bar{V}_t$	$S_{V,t}$	SN_t
	$k=1$	$k=2$	$k=3$	$k=4$	$k=5$	$k=6$	$k=7$			
0	-	-	-	-	-	-	-			
1	-0.01	-0.04	0.08	-0.08	0.03	-0.02	0.08	0.01	0.06	-1
2	-0.05	0.01	0.01	0.06	0.00	0.00	0.11	0.02	0.05	3
3	0.06	-0.05	-0.01	-0.03	0.04	0.05	0.07	0.02	0.05	1
4	0.03	-0.02	0.02	0.04	0.02	-0.01	0.08	0.02	0.03	3
5	0.02	0.07	0.01	0.03	0.01	0.01	0.08	0.03	0.03	7
6	0.11	0.10	0.08	0.10	0.11	0.04	0.06	0.09	0.03	7
7	0.08	0.11	0.12	0.12	0.13	0.12	0.06	0.11	0.03	7
8	0.07	0.04	0.06	0.07	0.07	0.05	0.07	0.06	0.01	7
9	0.04	0.01	0.01	0.00	-0.02	0.03	0.08	0.02	0.03	4
10	-0.01	0.04	0.02	0.00	0.01	0.01	0.14	0.03	0.05	4

Table 9: Phase II sample of the small shift data of manufacturing example

t	$X_{t,j}-\theta_0$												SN_t	CEWMA-1		CEWMA-1		CAEWMA	
	$j=1$	$j=2$	$j=3$	$j=4$	$j=5$	$j=6$	$j=7$	$j=8$	$j=9$	$j=10$	$j=11$	$j=12$		Y_t	R_t	Y_t	R_t	Y_t	R_t
0	-	-	-	-	-	-	-	-	-	-	-	-	-	0	0	0	0	0	0
1	-0.75	0.74	0.81	0.18	0.96	-1.21	0.21	0.81	0.29	-2.38	-0.17	1.42	4	2	4	0	12	0	8
2	0.42	0.94	-0.53	2.10	2.26	-0.21	1.37	-0.63	-1.37	0.15	0.26	-0.10	2	2	4	0	18	1	3
3	-0.04	-0.63	1.35	-0.38	0.40	-0.13	-0.76	-0.47	0.01	1.59	-0.65	1.67	-2	0	0	0	12	0	6
4	0.60	0.52	0.29	-0.61	0.21	-0.98	-2.08	-1.25	1.35	0.97	-0.91	1.33	2	1	2	0	18	1	1
5	1.33	-0.37	-0.34	-0.77	1.15	-1.14	-1.76	0.75	-0.64	-0.04	1.65	-0.56	-4	-1	-9	0	6	0	0
6	0.78	0.74	0.90	-0.88	-1.66	0.01	0.65	0.60	0.28	-0.14	1.23	0.77	4	1	2	0	18	0	8
7	-0.55	-0.45	-0.48	-0.56	-0.29	-0.39	0.13	1.86	-0.06	-0.62	1.82	-0.27	-6	-2	-11	0	0	0	-4
8	-0.99	-0.96	-1.85	0.61	-1.06	-0.09	0.13	-0.87	1.16	0.45	0.52	0.76	0	-1	-9	0	0	0	-4
9	-0.42	0.01	-1.33	-0.24	-0.24	-1.23	0.34	0.37	-0.96	1.35	0.80	-2.03	-2	-2	-4	0	-6	0	-8
10	-1.26	0.69	0.09	-1.14	0.46	0.08	0.30	0.55	-0.66	0.04	1.19	1.21	6	2	4	0	12	0	4
11	-0.13	-0.31	1.84	0.53	-1.21	-1.28	1.27	-0.45	0.12	-0.06	-0.06	0.94	-2	0	0	0	6	0	0
12	0.23	0.03	-0.04	0.81	0.83	1.18	1.11	-0.33	1.18	1.01	-0.22	-0.39	4	2	4	0	18	0	8
13	-1.40	1.12	0.13	-0.27	0.64	-0.94	1.87	-0.13	0.09	-1.00	1.08	2.42	2	2	4	1	2	1	3
14	2.17	0.04	0.29	-0.41	1.46	1.11	0.63	-0.47	-0.16	-0.53	-0.39	-0.12	0	1	2	0	21	1	1
15	-1.00	-1.33	1.29	1.54	-0.27	-0.22	0.83	0.54	-0.87	0.96	1.44	-0.44	0	0	7	0	21	0	8
16	1.37	-0.46	1.01	1.59	0.64	0.46	0.46	1.57	4.39	-0.14	-0.45	0.75	6	4	1	1	17	2	2
17	-0.86	1.46	1.26	0.92	2.87	0.39	0.06	-0.58	0.87	0.88	-0.38	-0.55	4	4	1	2	4	2	6
18	0.13	0.88	-0.31	1.10	0.19	0.98	-0.61	0.70	1.52	0.27	0.24	0.76	8	6	5	3*	0	4*	0
19	-0.11	-0.10	1.26	-1.30	-0.04	0.56	0.89	-0.77	-0.06	0.91	-0.39	-0.37	-4	0	7				
20	0.20	0.69	-0.81	0.18	-0.51	1.76	0.73	-0.20	-0.41	0.32	-0.24	0.35	2	1	9				
21	-0.40	2.35	1.46	0.85	0.78	-0.73	-0.94	3.19	-0.23	-0.44	-0.08	0.67	0	1	2				
22	0.43	1.03	1.35	0.72	0.56	0.58	1.04	0.29	0.61	0.73	0.01	-0.07	10	6	5				
23	-0.13	1.10	0.34	1.26	0.01	0.61	-0.19	4.05	3.34	0.22	-0.33	0.62	6	6	5				
24	-0.04	0.42	0.65	1.33	0.18	0.65	0.07	1.38	0.16	1.52	1.64	-0.82	8	7*	7				
25	-0.47	1.53	2.27	0.25	0.91	-0.67	0.06	0.41	-1.20	-0.96	-0.28	0.38	2						
26	0.47	-0.96	1.79	1.25	1.45	1.26	1.09	1.80	-0.13	1.52	-0.50	0.36	6						
27	0.49	-0.19	2.11	-0.32	0.15	-0.43	0.40	-0.69	-0.35	0.25	-0.51	-0.23	-2						
28	-0.01	3.29	-0.14	2.10	0.61	-0.18	-0.43	1.17	0.63	2.00	-1.25	0.78	2						
29	2.34	2.25	-0.34	0.16	2.34	0.34	-0.52	0.01	0.99	0.83	1.72	0.96	8						
30	1.65	-0.43	0.53	1.89	-0.63	0.50	0.67	1.65	3.58	-0.05	-1.09	0.36	4						

* Out-of-control signal

Table 10: Phase II sample of the large shift data of manufacturing example

t	$X_{t,j}-\theta_0$												SN_t	CEWMA-1		CEWMA-1		CAEWMA	
	$j=1$	$j=2$	$j=3$	$j=4$	$j=5$	$j=6$	$j=7$	$j=8$	$j=9$	$j=10$	$j=11$	$j=12$		Y_t	R_t	Y_t	R_t	Y_t	R_t
0	-	-	-	-	-	-	-	-	-	-	-	-	-	0	0	0	0	0	0
1	0.36	-0.28	-1.10	-0.72	0.73	0.52	-1.34	-0.53	-0.05	1.16	-0.33	1.32	-2	-1	-2	0	-6	0	-4
2	-0.62	0.52	0.18	0.52	-0.29	0.63	0.45	-0.16	-1.44	0.36	0.41	-0.15	2	0	7	0	0	0	0
3	-1.20	-1.33	-0.34	0.01	-1.16	0.88	-1.39	-0.12	0.87	-0.24	-0.16	1.78	-4	-1	-9	0	-12	0	-8
4	0.86	0.31	-0.93	0.32	-1.20	-0.08	1.67	0.57	2.87	0.69	-0.74	-0.33	2	0	0	0	-6	0	-4
5	0.29	-1.48	0.37	1.80	1.22	0.41	-1.13	-0.54	0.38	0.46	-0.35	-0.74	2	1	2	0	0	0	0
6	-0.19	1.06	0.14	-0.27	0.43	0.57	1.37	-2.50	-0.50	1.25	0.83	-0.33	2	1	9	0	6	0	4
7	0.43	-1.45	-1.49	-1.95	-0.25	1.92	-0.92	-0.11	0.26	-0.57	-0.57	-2.55	-6	-2	-4	0	-12	0	-8
8	-0.52	0.81	1.47	0.56	0.69	0.12	0.17	0.75	-0.68	0.03	0.09	-0.81	6	2	4	0	6	0	4
9	-0.70	-0.84	-1.87	-0.48	-1.31	-0.87	0.90	-0.81	-0.03	-2.16	0.46	-1.11	-8	-3	-6	0	-18	-1	-3
10	0.37	-1.05	-0.19	-0.86	-0.01	1.40	0.51	-1.63	-0.14	-0.18	1.04	-2.11	-4	-4	-1	-1	-8	-2	0
11	3.25	1.17	2.72	0.98	1.34	1.82	1.08	0.86	1.03	2.80	1.93	1.31	12	5	3	0	9	5*	0
12	1.06	2.01	1.97	-0.03	0.87	2.85	2.04	0.43	1.53	3.30	2.16	2.43	10	8*	2	1	17		
13	1.65	0.33	0.51	0.96	3.11	0.09	1.10	1.27	0.80	2.05	2.81	1.27	12			3*	6		
14	1.67	1.73	3.80	1.39	0.59	1.33	2.56	1.47	0.98	2.12	2.02	0.90	12						
15	3.32	-0.18	1.49	1.47	1.49	0.98	2.47	3.56	-0.20	2.27	1.11	1.88	8						

* Out-of-control signal

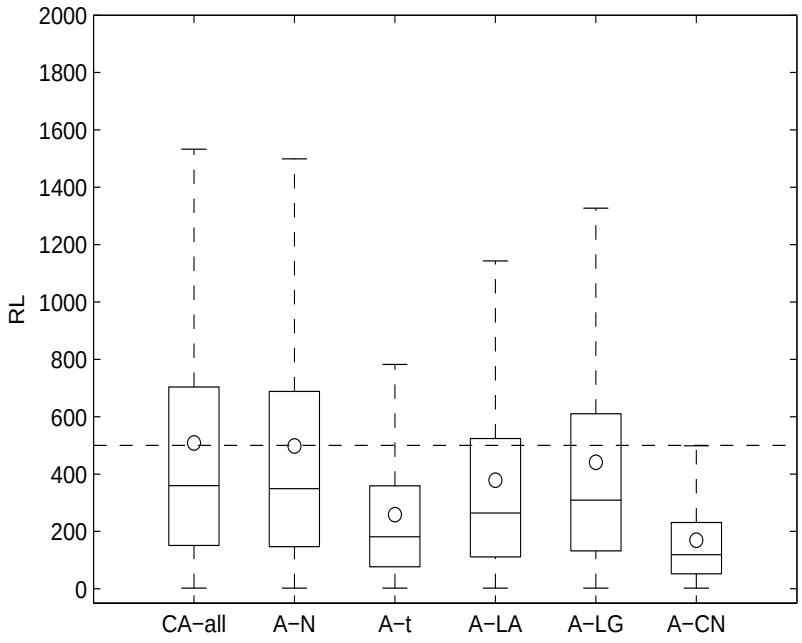

Figure 1: Boxplot-like graphs of the in-control RL distributions of the CAEWMA SN chart (first boxplot on the left) and the AEWMA $\bar{X}$ chart (remaining 5 boxplots on the right) when $n = 10$

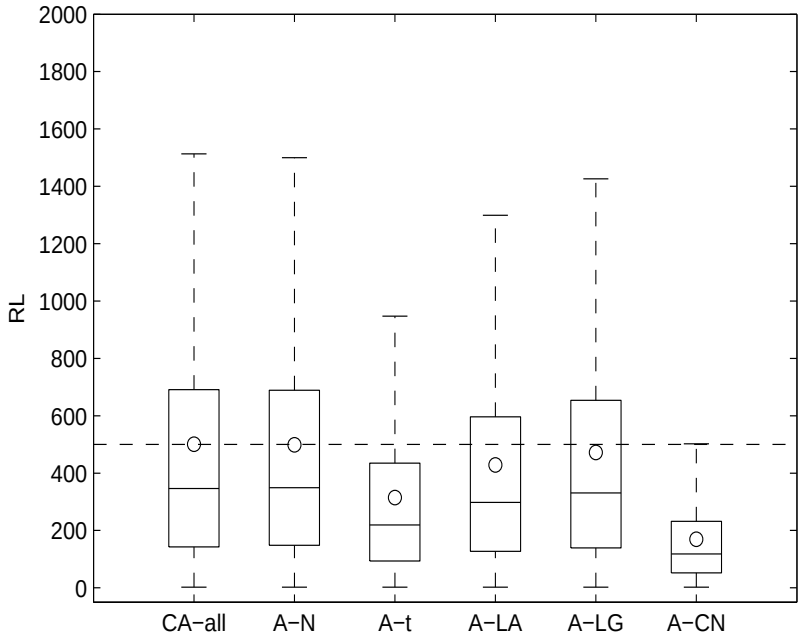

Figure 2: Boxplot-like graphs of the in-control RL distributions of the CAEWMA SN chart (first boxplot on the left) and the AEWMA $\bar{X}$ chart (remaining 5 boxplots on the right) when $n = 20$

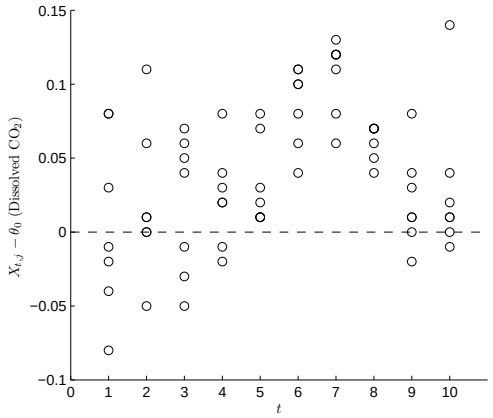

(a) Data in Table 8

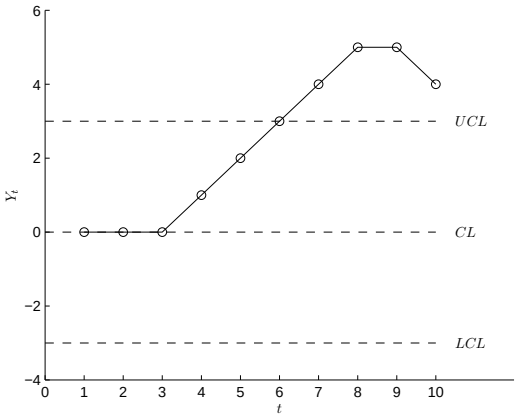

(b) CEWMA

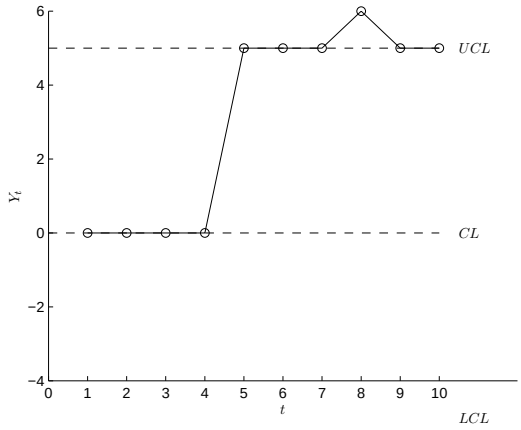

(c) CAEWMA

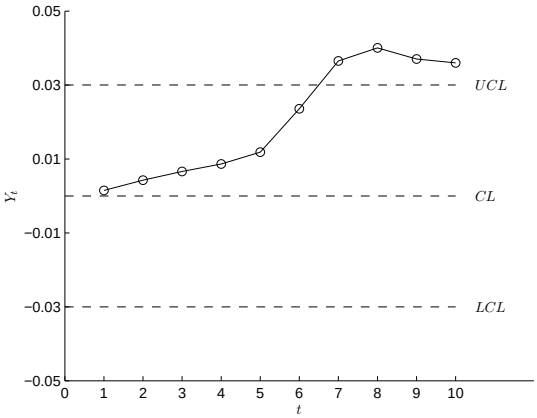

(d) AEWMA $\bar{X}$

Figure 3: Control charts applied to the beverage example

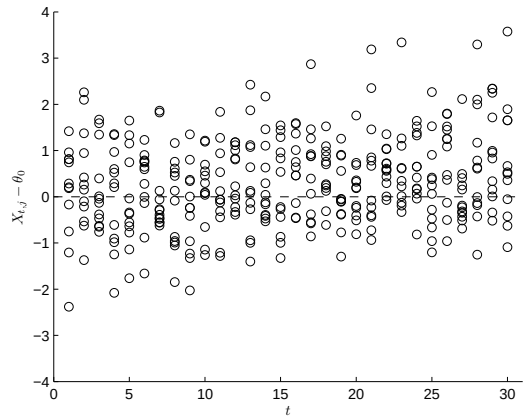

(a) Data in Table 9

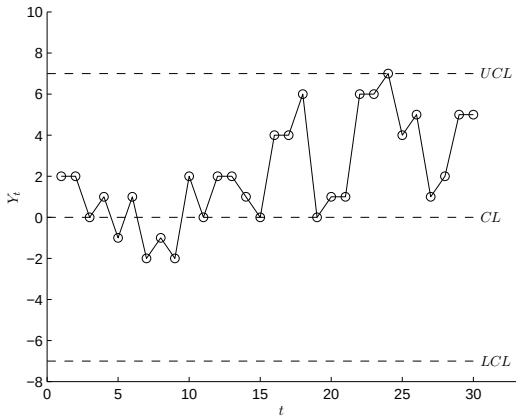

(b) CEWMA-1

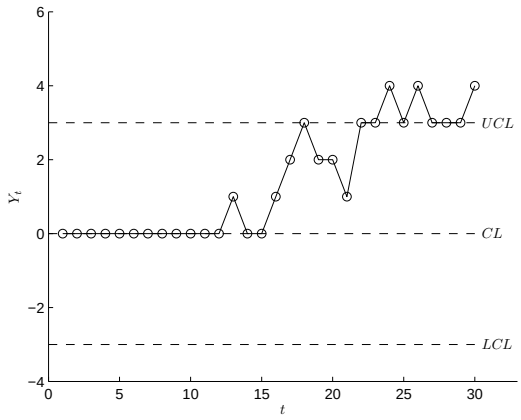

(c) CEWMA-2

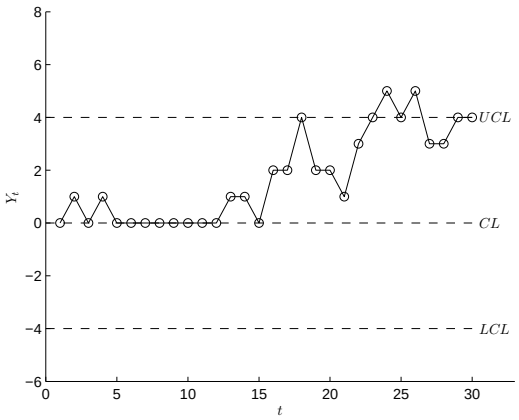

(d) CAEWMA

Figure 4: Control charts applied to the small shift data of manufacturing example

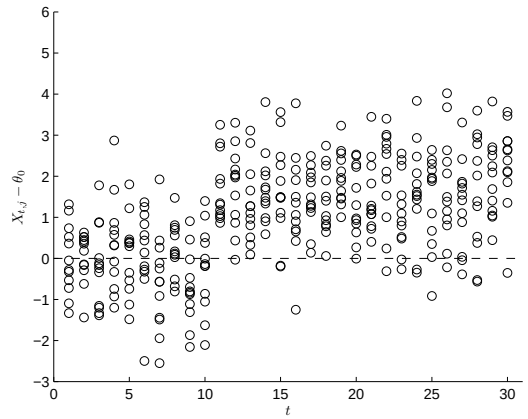

(a) Data in Table 10

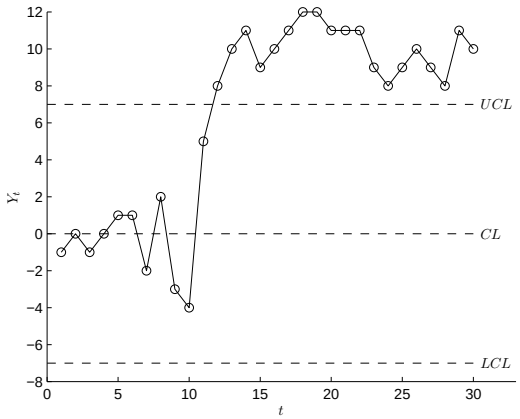

(b) CEWMA-1

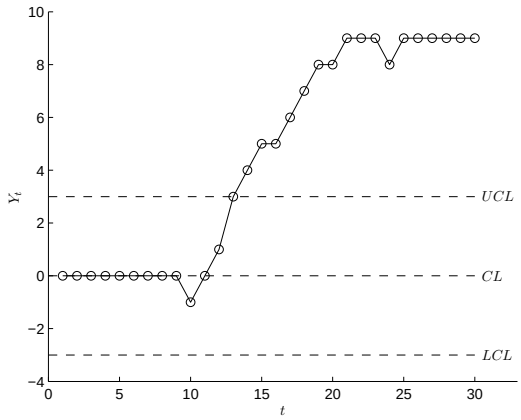

(c) CEWMA-2

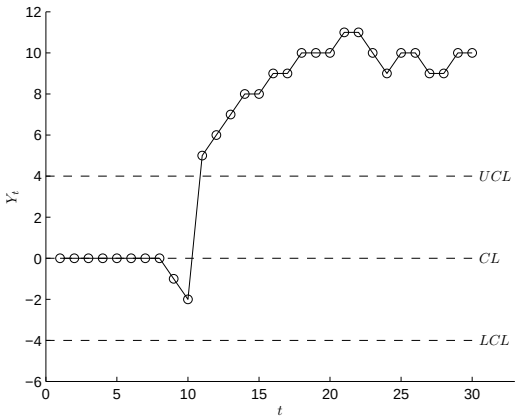

(d) CAEWMA

Figure 5: Control charts applied to the large shift data of manufacturing example